Conductance through contact barriers of a finite length quantum wire

Siddhartha Lal[1], **Sumathi Rao**[2] **and Diptiman Sen**[1]

[1] *Centre for Theoretical Studies*
Indian Institute of Science, Bangalore 560012, India

[2] *Harish-Chandra Research Institute*
Chhatnag Road, Jhusi, Allahabad 211019, India

Abstract

We use the technique of bosonization to understand a variety of recent experimental results on the conductivity of a quantum wire. The quantum wire is taken to be a finite-length Luttinger liquid connected on two sides to semi-infinite Fermi liquids through contacts. The contacts are modeled as (short) Luttinger liquids bounded by localized one-body potentials. We use effective actions and the renormalization group to study the effects of electronic interactions within the wire, the length of the wire, finite temperature and a magnetic field on the conductivity. We explain the deviations of the conductivity away from $2Ne^2/h$ in wires which are not too short as arising from renormalization effects caused by the repulsive interactions. We also explain the universal conductance corrections observed in different channels at higher temperatures. We study the effects of an external magnetic field on electronic transport through this system and explain why odd and even spin split bands show different renormalizations from the universal conductance values. We discuss the case of resonant transmission and of the possibility of producing a spin-valve which only allows electrons of one value of the spin to go through. We compare our results for the conductance corrections with experimental observations. We also propose an experimental test of our model of the contact regions.

PACS number: 72.10.-d, 85.30.Vw, 71.10.Pm, 73.40.Cg

1 Introduction

With the rapid advances made in the fabrication of high mobility semiconductor heterojunctions, these systems have provided the setting for the discovery of several new phenomena in quantum systems. Popular examples include mesoscopic systems like quantum dots, quantum wires, and the two-dimensional electron gas samples in which the quantum Hall effects are observed [1]. In particular, quantum wires are created by the electrostatic gating of two-dimensional electron gases (2DEG) (with typical densities of $n_{2DEG} \sim 0.5 - 6 \times 10^{15} m^{-2}$) in the inversion layer of GaAs heterostructures. These GaAs samples typically have a very high mobility (typically, $\mu \sim 3 - 8 \times 10^2 m^2 V^{-1} s^{-1}$) because there is very little disorder in them; the mean free path of an electron in the 2DEG is of the order of $\lambda_{MF} \sim 5 - 20 \mu m$. This makes it possible to create ballistic channels a few microns in length for studying electron transport in such wires, especially at low temperatures when the thermal de Broglie wavelength of the electron is comparable to the channel length. Furthermore, since it is possible to maintain a low carrier concentration in these wires, it becomes possible for transport to take place through only a few channels or even a single channel.

Thus, several observations [2-12] of the quantization of the conductance in electron transport through such channels have been made over the last two decades. More recently, several new ways have been found to produce such channels and this has led to even more precise experimental studies. This has brought into focus novel aspects of electron transport in such channels, not all of which are understood as yet.

Let us first briefly review some of the recent experimental findings in quantum wires. The first striking observation is that of a number of flat plateaus in the dc conductance which are separated by steps of roughly the same value [4]

$$g = N\tilde{g}\ \frac{2e^2}{h}\ , \tag{1}$$

where N denotes positive integers starting from one. The factor $\tilde{g} < 1$ and is found to vary with the length of the quantum wire and the temperature; it has been seen to be as low as 0.75. In fact, the plateaus tend towards $N(2e^2/h)$ as either the temperature is raised or the length of the quantum wire is shortened [3, 4]. This seems to imply a uniform renormalization of the plateau heights for each channel in the quantum wire as a function of wire length and temperature [4, 6, 8, 12]. Also, the flatness of the plateaus appears to indicate an insensitivity to the electron density in the channel. Furthermore, kinks are observed on the rise of the conductivity to some of the lowest plateaus. One such kink has been named the "0.7 effect" [5, 7, 12]. These kinks are seen to wash away quickly with increasing temperature [5, 7] and an external magnetic field placed in-plane and parallel to the channels [7]. Also, upon increasing such a magnetic field, a splitting of the

conductance steps is observed together with an *odd-even* effect of the renormalization of the plateau heights, with the odd and even plateau heights being renormalized by smaller and larger amounts respectively. Finally, at very high magnetic field, another kink is seen to arise near the first spin-split plateau.

Several of these experimental observations have found no satisfactory explanation till date. It is the purpose of this work to provide a consistent framework within which most of these observations of transport in quantum wires can be explained. We will rely upon several concepts and techniques that have become popular in the study of interacting mesoscopic systems. These include the concept of bosonization, effective actions and the renormalization group (RG) [13, 14, 15]. To be precise, we will employ these techniques and ideas to understand the low energy transport properties of ballistic electrons in a finite quantum wire attached to two semi-infinite Fermi leads [16, 17, 18], but with a difference; the contacts of the quantum wire with its leads will themselves be modeled as short quantum wires with junction barriers at either end. The properties of the contacts are unaffected by the external gate voltage which causes the formation of the discrete subbands in the quantum wire. The junction barriers will be modeled as localized δ-functions to account for the back-scattering of electrons due to the imperfect coupling between the quantum wire and the 2DEG reservoirs; these barriers will renormalize the conductance as observed in the experiments. We will also study the effect of external electric and magnetic fields on this system. The properties of such a model for the quantum wire will be seen to account for several of the experimental observations mentioned above, as well as predict the possibility of some more interesting observations in future experiments in these systems. It should be stated here that a possible mechanism for some of the experimental observations [4] has been proposed in Ref. [19]; this is based on the anomalously enhanced back-scattering of electrons entering the 2DEG reservoir from the quantum wire due to the formation of Friedel oscillations of the electron density near the edges of the reservoirs, and it neglects interactions between the electrons in the quantum wire. Our model, however, attempts to understand these observations keeping in mind the importance of electron-electron interactions, barrier back-scattering, finite temperature and magnetic field as well as all length scales in the quantum wire system.

The paper is organized as follows. In Sec. 2, we discuss the basics of the model outlined above. We show that the model can be described by a K_L-K_C-K_W Luttinger model [20] with three different interaction parameters in the lead (K_L), the contacts (K_C) and the wire (K_W). By assuming that the electron-electron interactions get screened out rapidly as one goes from one region to another, we get in a natural way the existence of localized barriers at the junctions. We then discuss how our model goes beyond the concept of *ideal* contact resistances as studied in the Landauer-Buttiker formalism. In Sec. 3, we study the effective action of our model in the presence of external electric fields after integrating

out all bosonic fields except those at the boundaries between the various regions - the leads, the contacts and the wire. Depending on the relative sizes of the contacts and the wire, we define two regimes - a) the quantum wire (QW) limit, where the length of the wire is much greater than the contact, and b) the quantum point contact (QPC) limit, where the length of the contacts is much greater than the length of the wire. We then study the symmetries of the effective action to determine when resonant transmission is possible as a function of a tunable gate voltage. All of this is first done for spinless fermions and subsequently, we give the modifications of the results for spinful fermions. In Sec. 4, we explicitly compute the corrections to the conductance due to the barriers at finite temperature (T) and for a finite length of the wire (l) and for finite contact lengths (d). We compute the frequency dependent Green's functions of the model, in the different frequency regimes and use the Kubo formula to compute the conductance. We also show how these results could have been anticipated from the renormalization group (RG) equations for the barrier strengths. In Sec. 5, we study our model in the presence of an external in-plane magnetic field. Using RG methods, we show that the spin-up and spin-down electrons see different barrier heights at the junctions, and use this idea to explain the odd-even effect mentioned earlier. We also outline all the possible resonances that can be seen under such conditions. We point out the possibility of producing a spin-valve at moderate magnetic fields. In addition, we compute the conductance of our model and discuss its qualitative features as a function of the strength of the magnetic field. In Sec. 6, we compare the features of the conductance expressions obtained with the observations made in various experiments for transport in quantum wires with and without an external magnetic field. We find that our model is applicable to a large class of experiments and gives a unified and qualitatively correct explanation of all of them. In particular, our model gives a possible explanation for the uniform renormalization of all the conductance steps seen in several experiments. We also explain the odd-even effect seen in experiments in the presence of magnetic field. In addition, we propose more precise experimental tests of our model. Finally, we end in Sec. 7, with a summary of all the new results in our paper, and outline further investigations that are possible.

2 The Model

In this section, we will study the Tomonaga-Luttinger liquid (TLL) model [13] of a quantum wire of finite length with no disorder, which is connected to the two 2DEG reservoirs modeled as two semi-infinite Fermi leads through two contact regions. The contacts are modeled as short quantum wires with the junctions at either end modeled as δ-function barriers. The inter-electron interactions in the system, and hence the parameter K which characterizes the interactions, vary abruptly at each of the junctions. Hence, we study

a K_L-K_C-K_W-K_C-K_W model (see Fig. 1). The motivation for the above model is as follows. The electrons in the 2DEG are basically free, and hence, in the equivalent 1D model, they are modeled as semi-infinite leads with Luttinger parameter $K_L = 1$. This can be understood as follows: if each end of the quantum wire is approximated by a point, only those electrons in the 2DEG which are in a zero angular momentum state (with respect to the appropriate end) can enter (or leave) the wire. Thus, the wave function of such a state has the radial coordinate as its only variable and we may, therefore, model the 2DEG as noninteracting 1D systems lying on either side of the quantum wire. The electron velocity in the leads v_L is given by the Fermi velocity of the 2DEG electrons in the reservoirs $v_F = \sqrt{2E_{F2D}/m}$. On the other hand, the externally applied gate voltage V_G is applied over a small region and this leads to the formation of several discrete sub-bands where the electrons feel the transverse confinement potential produced by V_G. This region is the one-dimensional quantum wire where the density of electrons is controlled by the gate voltage. The lowest energies E_s in each sub-band are given by the discrete energy levels for the transverse confinement potential (and can therefore be shifted by changing V_G) [21]. The Fermi energy in the s^{th} channel is given by $E_{F1D} = E_{F2D} - E_s$. A channel is open when $E_{F1D} > 0$; the electron velocity $v_W(e)$ in the channel is then related to the 2DEG Fermi velocity v_F by $v_W(e) = \sqrt{v_F^2 - 2E_s/m}$. In this gate voltage constricted region, the electrons will be considered as interacting via a short range (Coulomb-like) repulsion. Thus each discrete channel is modeled by a separate TLL. Let us, for the moment, consider one such channel with an interaction parameter K_W and quasiparticle velocity v_W.

The contacts represent the regions where the geometry changes from two-dimensional (2D) to 1D. In these regions of changing geometry, interactions between the electrons are likely to be very important; thus we model the contact region as a Luttinger liquid with $K = K_C$. However, the gate voltage V_G is unlikely to affect the properties of the electrons in these regions as the discrete sub-bands form a little deeper inside the wire. We choose different parameters K_W for the wire and K_C for the contact, because it is not obvious that inter-electrons interactions within the quantum wire will be the same as in the contact. The density of electrons in the quantum wire is controlled by the gate voltage, whereas the density of electrons in the contacts is controlled by the density of the 2DEG at or near the Fermi energy. Hence, we expect K_C to be independent of V_G, but K_W is dependent on E_{F1D}, which, in turn depends on V_G. We will also show below that the change in the inter-electron interactions in each of the lead, contact and quantum wire regions gives rise to barrier-like back-scattering of the electrons.

Simpler versions of this model (but without junction barriers and without contacts) have been studied by several authors [16, 17, 18] who found perfect conductance through the TLL channel which is independent of the inter-electron interactions. Perfect con-

ductance is also seen in several of the experiments [2, 3, 4, 5, 7]. In the opposite limit, the model of a finite quantum wire connected to the two reservoirs by tunneling through very large barriers has also been studied [22]. The idea of modeling 2DEG reservoirs by 1D noninteracting Fermi leads has also earlier been employed in studies of the fractional quantum Hall effect edge states coupled to Fermi liquids through a tunneling term in the Hamiltonian [23]. Some studies of disordered quantum wires in such a model (again with perfect junctions) have also been conducted and the corrections to the conductance because of back-scattering impurities found [24, 27]. The continuity of the results found in these studies (which have quantum wires of a finite length) with those found earlier for infinite quantum wires [14] has also been established [18, 24].

The main difference between our model and the earlier studies of the quantum wire is that here we explicitly model the contacts as short TLL wires bounded by junction barriers on either end and whose properties are unaffected by the gate voltage V_G. As we will discuss later, an experiment performed recently [9] has conclusively shown the existence of a region (of an appreciable length of $2 - 6\mu m$) in between the quantum wire and the 2DEG reservoirs which leads to the back-scattering of 2DEG electrons entering the quantum wire. Furthermore, the idea that the properties of a one-dimensional system are determined by the Fermi energy of the 2DEG reservoirs has been used in Ref. [25] to study the quantum point contact. In addition, we assume that the changes in the inter-electron interactions take place abruptly in going from the contacts into the quantum wire and that all inter-electron interactions get screened out very quickly in going from the contacts into the leads. It can, however, be shown that a smoother variation of the interaction parameter K upon going from the quantum wire into the contacts and in going from the contacts into the noninteracting leads does not affect any of the transport properties in the $\omega \to 0$ (dc) limit as long as we have no barriers of any kind in the system. We will now show that changes in the inter-electron interactions at the lead-contact and contact-quantum wire junctions give rise to barrier-like terms in the Hamiltonian of the system; the existence of these terms is mentioned briefly in the work of Safi and Schulz [24]. This is, however, only one reason why the junctions between the 1D channel and its leads can cause the back-scattering of electrons; another reason is clearly the change in geometry in going from the 2DEG reservoirs into the 1D channel. This cause for the drop in the conductance of the channel has earlier been studied within the purview of the Landauer-Buttiker formalism; see [26] and references therein.

Let us begin by studying the simpler case of a quantum wire (in which electrons are interacting with each other) connected directly to the noninteracting, semi-infinite leads without any intermediate contact regions. Then there is only a single change in inter-electron interactions from zero in the leads to a finite value in the quantum wire. The kinetic part of the Hamiltonian for this system of interacting spinless electrons in

the quantum wire when expressed in terms of the bosonic field $\phi(x)$ and its canonically conjugate momentum $\Pi(x) = \partial_t \phi / v_F$ is given by

$$H_0 = \frac{1}{2} \int dx v_F [\Pi(x)^2 + (\partial_x \phi(x))^2] \ , \tag{2}$$

where v_F is the Fermi velocity of the electrons in the channel. The part of the Hamiltonian which characterizes the short-ranged density-density interactions between the electrons in a 1D channel of length l is given by

$$H_{int} = \int_0^l dx \int_0^l dy \, \mathcal{U}(x,y) \rho(x) \rho(y) \ , \tag{3}$$

where $\mathcal{U}(x,y)$ characterizes the strength of the density-density interactions between the electrons, and $\rho(x)$ is the electronic density at the point x. Using a truncated form of the Haldane representation for the electronic density in terms of the bosonic field $\phi(x)$ [13], the density $\rho(x)$ is given by

$$\rho(x) = \frac{1}{\sqrt{\pi}} \partial_x \bar{\phi}(x) \ [c_0 + 2c_1 \cos(2\sqrt{\pi}\bar{\phi}(x))] \ , \tag{4}$$

where $\bar{\phi}(x) = \phi(x) + k_F x / \sqrt{\pi}$, $c_0 = 1$, $c_1 = \Lambda/(2k_F)$, and k_F is the Fermi wave vector. Λ is the ultraviolet cutoff ($\Lambda < O(E_{F1D})$); it is the energy limit up to which the linearization of the bands and hence bosonization is expected to be applicable. If we now characterize the short range inter-electron interactions by $\mathcal{U}(x,y) = \mathcal{U}_0 \delta(x-y)$, then we can substitute the expressions for the density and the inter-electron interaction into the interaction term in the Hamiltonian. This gives us

$$\begin{aligned}
H_{int} &= \mathcal{U}_0 \int_0^l dx \ [\{\partial_x (\frac{c_0}{\sqrt{\pi}} \bar{\phi})\}^2 \ - \ 2\partial_x (\frac{c_0}{\sqrt{\pi}} \bar{\phi}) \partial_x (\frac{c_1}{\sqrt{\pi}} \sin(2\sqrt{\pi}\bar{\phi})) \\
&\qquad + \ \{\partial_x (\frac{c_1}{\sqrt{\pi}} \sin(2\sqrt{\pi}\bar{\phi}))\}^2] \\
&= \mathcal{U}_0 \int_0^l dx \ [\frac{c_0^2}{\pi} (\partial_x \bar{\phi})^2 \ + \ 2\frac{c_0^2 k_F}{\pi} \partial_x \phi \ + \ 2\frac{c_0 c_1 k_F}{\sqrt{\pi}} \partial_x \sin(2\sqrt{\pi}\bar{\phi}) \\
&\qquad + \ 2\frac{c_0 c_1}{\sqrt{\pi}} \partial_x \phi \partial_x \sin(2\sqrt{\pi}\bar{\phi}) \ + \ 2\frac{c_1^2}{\pi} (\partial_x \bar{\phi})^2 (\cos(4\sqrt{\pi}\bar{\phi}) + 1)] \\
&= \mathcal{U}_0 \int_0^l dx \ [(\frac{c_0^2 + 2c_1^2}{\pi}) (\partial_x \phi)^2 \ + \ 2k_F (\frac{c_0^2 + 2c_1^2}{\pi}) \partial_x \phi \ + \ 2\frac{c_0 c_1 k_F}{\sqrt{\pi}} \partial_x \sin(2\sqrt{\pi}\bar{\phi}) \\
&\qquad + \ 2\frac{c_0 c_1}{\sqrt{\pi}} \partial_x \phi \partial_x \sin(2\sqrt{\pi}\bar{\phi}) \ + \ 2\frac{c_1^2}{\pi} (\partial_x \bar{\phi})^2 \cos(4\sqrt{\pi}\bar{\phi})].
\end{aligned} \tag{5}$$

We can now simplify this expression by noting that several of the terms above contain rapidly oscillating factors of $\cos(k_F x)$ or $\sin(k_F x)$ which make those terms vanish upon performing the integration (unless we are at very specific fillings of the electron density). Thus, we can ignore the fifth term straightaway. The first term can be added to a similar term in H_0 where it renormalizes the velocity and introduces an interaction parameter K. The second term is a chemical potential term and that too can be accounted for by shifting the field ϕ accordingly. The third term is clearly a boundary term, and it gives us two barrier like terms at $x = 0$ and $x = l$, with

$$\begin{aligned} H_{barrier} &= 2\mathcal{U}_0 \frac{c_0 c_1 k_F}{\sqrt{\pi}} \int_0^l dx\ \partial_x \sin(2\sqrt{\pi}\bar{\phi}) \\ &= 2\mathcal{U}_0 \frac{c_0 c_1 k_F}{\sqrt{\pi}} \left[\sin(2\sqrt{\pi}\phi(l) + 2k_F l) \ - \ \sin(2\sqrt{\pi}\phi(0))\right]. \end{aligned} \tag{6}$$

Finally, the fourth term can also be rewritten as

$$\begin{aligned} H_{int,4} &= 4\mathcal{U}_0 \frac{c_0 c_1}{\sqrt{\pi}} \int_0^l dx\ (\partial_x \phi)^2 \cos(2\sqrt{\pi}\bar{\phi}) \ + \ 2\mathcal{U}_0 \frac{c_0 c_1 k_F}{\sqrt{\pi}} \int_0^l dx\ \partial_x \sin(2\sqrt{\pi}\bar{\phi}) \\ &\quad - 4\mathcal{U}_0 \frac{c_0 c_1 k_F^2}{\sqrt{\pi}} \int_0^l dx\ \cos(2\sqrt{\pi}\bar{\phi}) \ , \end{aligned} \tag{7}$$

in which the first and third terms again vanish because they contain rapidly oscillating factors within the integrals, and the second term adds on to $H_{barrier}$ exactly. All this finally gives us two δ-function barriers at the junctions of the quantum wire with its Fermi liquid leads as

$$H_{barrier} = 4\mathcal{U}_0 \frac{c_0 c_1 k_F}{\sqrt{\pi}} \left[\sin(2\sqrt{\pi}\phi(l) + 2k_F l) \ - \ \sin(2\sqrt{\pi}\phi(0))\right] \ . \tag{8}$$

The extension of the derivation given above to our model with two intermediate contact regions where the inter-electron interactions are $\mathcal{U}(x, y) = \mathcal{U}_1 \delta(x - y)$ (i.e., different from that in the quantum wire) is straightforward, and it yields four barrier terms: two at the junctions of the contacts with the leads, and two at the junctions of the contacts with the quantum wire. It is also very likely that the inner two barriers are much weaker than the outer two since the change in inter-electron interactions in going from the contacts to the quantum wire is likely to be much smaller than that in going from the contacts to the leads; also the change in geometry at the contact-quantum wire junction is likely to be much more adiabatic. Thus, we will from now on consider the junctions between the wire and the contacts and between the contacts and the leads as local barriers whose heights are determined by several factors, such as the nature of the inter-electron interaction and its screening, and the deviations from adiabaticity in the change in geometry in going

from the reservoirs into the contacts or from the contacts into the quantum wire. To be general, we should take these four barriers to have different heights but it is very likely that any asymmetry between the left two and right two contacts will be small. Thus, we can finally write the complete Hamiltonian for the quantum wire of spinless electrons, its contacts and its leads as

$$\begin{aligned} H &= (\int_{-\infty}^{0} + \int_{l+2d}^{\infty})\, dx\, \frac{v_F}{2}[\Pi(x)^2 + (\partial_x\phi(x))^2] \\ &\quad +(\int_{0}^{d} + \int_{l+d}^{l+2d})\, dx\, \frac{v_C}{2K_C}[\Pi_C(x)^2 + (\partial_x\phi(x))^2] \\ &\quad + \int_{d}^{l+d} dx\, \frac{v_W}{2K_W}[\Pi_W(x)^2 + (\partial_x\phi(x))^2] + V_{LC}\sin(2\sqrt{\pi}\phi(0)) \\ &\quad +V_{CW}\sin(2\sqrt{\pi}\phi(d) + 2k_F d) + V_{WC}\sin(2\sqrt{\pi}\phi(l+d) + 2k_F(l+d)) \\ &\quad +V_{CL}\sin(2\sqrt{\pi}\phi(l+2d) + 2k_F(l+2d))\ , \end{aligned} \tag{9}$$

where $\Pi_{C,W}(x) = (1/v_{C,W})\partial_t\phi(x)$. Finally, it is worth commenting here that since our model shows that a quantum wire with no disorder already has back-scattering junctions built into it, the notion of *ideal contact resistances* (which are seen in a study of this system using the Landauer-Buttiker formalism and arise from the *ideal* connection of the quantum wire to its reservoirs) which are universal in value, $h/2e^2$ to be precise, does not seem to hold true even for the so-called clean quantum wire with adiabatic junctions in the presence of inter-electron interactions within the quantum wire. We will show later that these junction barriers are likely to be weak when the lengths of the quantum wires are quite short or temperatures are not very low, and that the junction barriers are likely to remain weak even after some small renormalization that might take place due to the electron-electron interactions in the quantum wire. Thus, the contact resistances between the wire and the reservoirs due to the junction barriers will be very nearly the universal value quoted above only for very short quantum wires (i.e., quantum point contacts) or when the temperatures are not very low. This is also observed in all the experiments till date [3, 4, 5, 7].

The generalization of the model to spinful fermions is straightforward. For completeness, we give below the Hamiltonian for spinful electrons in a quantum wire connected to external reservoirs through the contacts and junction barriers,

$$\begin{aligned} H_{spin} &= \sum_{i=\uparrow,\downarrow}\Big[(\int_{-\infty}^{0} + \int_{l+2d}^{\infty})\, dx\, \frac{v_{iF}}{2}[\Pi_i(x)^2 + (\partial_x\phi_i(x))^2] \\ &\quad +(\int_{0}^{d} + \int_{l+d}^{l+2d})\, dx\, \frac{v_{iC}}{2K_{iC}}[\Pi_{iC}(x)^2 + (\partial_x\phi_i(x))^2] \end{aligned}$$

$$+\int_d^{l+d} dx\ \frac{v_{iW}}{2K_{iW}}[\Pi_{iW}(x)^2+(\partial_x\phi_i(x))^2]+V_{iLC}\sin(2\sqrt{\pi}\phi_i(0))$$
$$+V_{iCW}\sin(2\sqrt{\pi}\phi_i(d)+2k_{iF}d)+V_{iWC}\sin(2\sqrt{\pi}\phi_i(l+d)+2k_{iF}(l+d))$$
$$+V_{iCL}\sin(\sqrt{\pi}\phi_i(l+2d)+2k_{iF}(l+2d))\Big]. \quad (10)$$

Note that we have allowed for independent velocities and interaction strengths for the $\uparrow$ and $\downarrow$ electrons. This generality will be required when we study the model in the presence of a magnetic field. Finally, let us note the fact that we will be taking into account only the outer two junction barriers (i.e., those at the junctions of the contacts and the leads) in all our subsequent calculations as these are likely to be the more significant junction barriers in the system as long as transport through fully open quantum wires is considered.

3 Effective Actions

In this section, the aim is to obtain an effective action in terms of the fields at the junction barriers for both spinless and spinful electrons. We then analyze the symmetries of the effective action and obtain the resonance conditions.

3.1 The case of spinless electrons

In Sec. 2, it was shown that the screening out of the interactions in the 2DEG leads to a Hamiltonian with junction barriers given in Eq. (9). The effective action for this model of spinless electrons can be written as

$$S = S_0 + S_{barrier} + S_{gate}\ , \quad (11)$$

where we have defined each of the actions separately below.

$$S_0 = \int d\tau\ [\int_{-\infty}^{0} dx\mathcal{L}_1 + \int_0^d dx\mathcal{L}_2 + \int_d^{l+d} dx\mathcal{L}_3 + \int_{l+d}^{l+2d} dx\mathcal{L}_2 + \int_{l+2d}^{\infty} dx\mathcal{L}_1]\ , \quad (12)$$

where

$$\mathcal{L}_1 = \mathcal{L}(\phi; K_L, v_L), \quad \mathcal{L}_2 = \mathcal{L}(\phi; K_C, v_C), \quad \text{and} \quad \mathcal{L}_3 = \mathcal{L}(\phi; K_W, v_W)\ , \quad (13)$$

and we have defined $\mathcal{L}(\phi; K, v) = (1/2Kv)(\partial_\tau\phi)^2 + (v/2K)(\partial_x\phi)^2$, and used the imaginary time $\tau = it$ notation.

$$S_{barrier} = \int d\tau\ \Lambda[V_1\cos(2\sqrt{\pi}\phi_1) + V_1\cos(2\sqrt{\pi}\phi_4 + 2k_FL)$$
$$+ V_2\cos(2\sqrt{\pi}\phi_2 + 2k_Fd) + V_2\cos(2\sqrt{\pi}\phi_3 + 2k_F(l+d))]\ , \quad (14)$$

where we have set $V_{LC} = V_{CL} = V_1\Lambda$ and $V_{CW} = V_{WC} = V_2\Lambda$ assuming left-right symmetric barriers (V_1 and V_2 are dimensionless), and have used $\phi(0,\tau) = \phi_1(\tau) \equiv \phi_1$, $\phi(d,\tau) = \phi_2(\tau) \equiv \phi_2$, $\phi(l+d,\tau) = \phi_3(\tau) \equiv \phi_3$ and $\phi(L,\tau) = \phi_4(\tau) \equiv \phi_4$. The total length of the wire is denoted by $L = l + 2d$. We shall henceforth assume that $V_2 \ll V_1$ and can be dropped; as we have explained earlier, the inner two barriers are likely to be weaker than the outer two barriers. We also include the coupling of the electrons in the wire to an external gate voltage V_G given by

$$S_{gate} \;=\; V_G \int d\tau \int_d^{l+d} dx \rho(x,\tau) \;=\; V_G \int d\tau \frac{[\phi_3 - \phi_2]}{\sqrt{\pi}}. \tag{15}$$

This coupling is necessary because it is the gate voltage which controls the density of electrons in the wire, which, in turn, controls the number of channels in the quantum wire. Experimentally, an external voltage drop across the wire drives the current through the wire, which is measured as a function of the gate voltage or the density of electrons in the wire.

Since the Luttinger liquid action is quadratic, the effective action can be obtained in terms of the fields ϕ_i, $i = 1...4$, by integrating out all degrees of freedom except those at the positions of the four junction barriers, following Ref. [14]. Using the (imaginary time) Fourier transform of the fields

$$\phi_1(\tau) = \sum_{\bar{\omega}_n} e^{-i\bar{\omega}_n\tau}\tilde{\phi}_{1n}(\bar{\omega}_n), \quad \phi_2(\tau) = \sum_{\bar{\omega}_n} e^{-i\bar{\omega}_n\tau}\tilde{\phi}_{2n}(\bar{\omega}_n)\ , \tag{16}$$

we explicitly obtain the S_0 part of the effective action; this is presented in Appendix A. (The $\bar{\omega}_n$ are the Matsubara frequencies which are quantized in multiples of the temperature as $\bar{\omega}_n = 2\pi n k_B T$). In the high frequency limit, or, equivalently at high temperatures, where $\bar{\omega}_n d/v_C, \bar{\omega}_n l/v_W \gg 1$, the effective action reduces to

$$S_{0,eff,high}(\tilde{\phi}_1,\tilde{\phi}_2,\tilde{\phi}_3,\tilde{\phi}_4) = \frac{K_L+K_C}{2K_LK_C}\sum_{\bar{\omega}_n}|\bar{\omega}_n|(\tilde{\phi}_1^2+\tilde{\phi}_4^2) + \frac{K_W+K_C}{2K_WK_C}\sum_{\bar{\omega}_n}|\bar{\omega}_n|(\tilde{\phi}_2^2+\tilde{\phi}_3^2). \tag{17}$$

In this limit, all the barriers are seen as the sum of individual barriers with no interference. In fact, if we integrate out the two inner fields ϕ_2 and ϕ_3, we are just left with

$$S_{0,eff,high}(\tilde{\phi}_1,\tilde{\phi}_4) = \frac{K_L+K_C}{2K_LK_C}\sum_{\bar{\omega}_n}|\bar{\omega}_n|(\tilde{\phi}_1^2+\tilde{\phi}_4^2). \tag{18}$$

The surprising point to note is that the effective interaction strength $K_{eff} = K_LK_C/(K_L+K_C)$ depends only on the interaction strengths in the contacts and in the leads (where there are no interactions), and not on the interaction strength in the wire! Furthermore,

since the gate voltage V_G couples only to the inner fields ϕ_2 and ϕ_3 and these two fields are completely decoupled from the outer fields ϕ_1 and ϕ_4 in $\mathcal{L}_{0,eff,high}(\phi_1,\phi_2,\phi_3,\phi_4)$ above, integrating out ϕ_2 and ϕ_3 does not lead to any gate voltage term in the final effective action in this temperature regime.

Depending on whether $d \gg l$ or $l \gg d$, we can have two possible scenarios of intermediate regimes, each with two crossovers. We can express all our lengths in terms of equivalent temperatures by defining $v_C/d = k_B T_d$ and $v_W/l = k_B T_l$. So the high temperature limit defined above is just $T \gg T_d, T_l$.

- Let us first consider the quantum wire limit where $l \gg d$.

  In the intermediate frequency (or temperature) regime of $T_l \ll T \ll T_d$, the action becomes

$$\begin{aligned} S_{0,eff,int}(\tilde{\phi}_1,\tilde{\phi}_2,\tilde{\phi}_3,\tilde{\phi}_4) &= \frac{1}{2K_L}\sum_{\bar{\omega}_n}|\bar{\omega}_n|(\tilde{\phi}_1^2+\tilde{\phi}_4^2)+\frac{1}{2K_W}\sum_{\bar{\omega}_n}|\bar{\omega}_n|(\tilde{\phi}_2^2+\tilde{\phi}_3^2) \\ &\quad +\frac{U_C}{2}\sum_{\bar{\omega}_n}[(\tilde{\phi}_1-\tilde{\phi}_2)^2+(\tilde{\phi}_3-\tilde{\phi}_4)^2]+S_{gate}, \end{aligned} \tag{19}$$

  where $U_C = v_C/(K_C d)$ is an energy whose significance will become clear shortly. As the action is quadratic, we can integrate out $\tilde{\phi}_2$ and $\tilde{\phi}_3$ to be left with an action dependent only on $\tilde{\phi}_1$ and $\tilde{\phi}_4$ as given by

$$\begin{aligned} & S_{0,eff,int}(\tilde{\phi}_1,\tilde{\phi}_4) \\ = \; & \frac{1}{2K_L}\sum_{\bar{\omega}_n}|\bar{\omega}_n|(\tilde{\phi}_1^2+\tilde{\phi}_4^2) \\ + \; & \frac{1}{2K_W}\sum_{\bar{\omega}_n}|\bar{\omega}_n|[\frac{U_C^2}{A^2}(\tilde{\phi}_1^2+\tilde{\phi}_4^2)+\frac{2\tilde{V}_G U_C}{A^2}(\tilde{\phi}_1-\tilde{\phi}_4)] \\ + \; & \frac{U_C}{2}\sum_{\bar{\omega}_n}\Big[[(\frac{U_C}{A}-1)\tilde{\phi}_1+\frac{\tilde{V}_G}{A}]^2+[(\frac{U_C}{A}-1)\tilde{\phi}_4-\frac{\tilde{V}_G}{A}]^2\Big] \\ + \; & \int d\tau \frac{\tilde{V}_G U_C}{A}(\phi_4-\phi_1)\ , \end{aligned} \tag{20}$$

  where $A = U_C + |\bar{\omega}_n|/K_W$ and $\tilde{V}_G = V_G/\sqrt{\pi}$. We can approximate A by U_C which is justified in the intermediate regime as $T \ll T_d$ and $K_C \sim K_W$. Then we are finally left with the expression

$$S_{0,eff,int}(\tilde{\phi}_1,\tilde{\phi}_4) = \frac{K_L+K_W}{2K_L K_W}\sum_{\bar{\omega}_n}|\bar{\omega}_n|(\tilde{\phi}_1^2+\tilde{\phi}_4^2) \; + \; \int d\tau \tilde{V}_G(\phi_4-\phi_1)\ . \tag{21}$$

- Now, we consider the QPC limit where $d \gg l$.

  In the regime where $T_d \ll T \ll T_l$, the action becomes

$$\begin{aligned} S_{0,eff,int}(\tilde{\phi}_1, \tilde{\phi}_2, \tilde{\phi}_3, \tilde{\phi}_4) &= \frac{1}{2K_L} \sum_{\bar{\omega}_n} |\bar{\omega}_n| (\tilde{\phi}_1^2 + \tilde{\phi}_4^2) \\ &+ \frac{1}{2K_C} \sum_{\bar{\omega}_n} |\bar{\omega}_n| (\tilde{\phi}_1^2 + \tilde{\phi}_2^2 + \tilde{\phi}_3^2 + \tilde{\phi}_4^2) \\ &+ \frac{U_W}{2} \sum_{\bar{\omega}_n} (\tilde{\phi}_2 - \tilde{\phi}_3)^2 + S_{gate}, \end{aligned} \tag{22}$$

  where $U_W = v_W/(K_W l)$ is again a frequency independent energy. As before, we can integrate out $\tilde{\phi}_2$ and $\tilde{\phi}_3$ to be left with an action dependent only on $\tilde{\phi}_1$ and $\tilde{\phi}_4$ given by

$$S_{0,eff,int}(\tilde{\phi}_1, \tilde{\phi}_4) = S_{0,eff,high}(\tilde{\phi}_1, \tilde{\phi}_4) \ . \tag{23}$$

  Thus there is no difference between the intermediate and high energy scales in the QPC limit because the gate voltage is applied over too short a length to affect the conductance even at intermediate temperatures.

Finally, in the low frequency limit where $\bar{\omega}_n \ll v_W/l, v_c/d$ (i.e., $T \ll T_d$ and $T \ll T_l$), S_0 reduces to

$$\begin{aligned} S_{0,eff,low}(\tilde{\phi}_1, \tilde{\phi}_2, \tilde{\phi}_3, \tilde{\phi}_4) &= \frac{1}{2K_L} \sum_{\bar{\omega}_n} |\bar{\omega}_n| (\tilde{\phi}_1^2 + \tilde{\phi}_4^2) + \frac{U_C}{2} \sum_{\bar{\omega}_n} [(\tilde{\phi}_1 - \tilde{\phi}_2)^2 + (\tilde{\phi}_3 - \tilde{\phi}_4)^2] \\ &+ \frac{U_W}{2} \sum_{\bar{\omega}_n} (\tilde{\phi}_2 - \tilde{\phi}_3)^2 \ . \end{aligned} \tag{24}$$

Since the action is still quadratic, it is possible to integrate out the two inner fields $\tilde{\phi}_2$ and $\tilde{\phi}_3$ and get the effective action wholly in terms of the $\tilde{\phi}_1$ and $\tilde{\phi}_4$ fields, remembering however, to also include the gate voltage term which couples to the inner fields. After doing out, we are left with the full effective action as

$$\begin{aligned} S_{eff,low}(\phi_1, \phi_4) &= S_{0,eff,low} + S_{gate} + S_{barrier} \\ &= \frac{1}{2K_L} \sum_{\bar{\omega}_n} |\bar{\omega}_n| (\tilde{\phi}_1^2 + \tilde{\phi}_4^2) + \frac{U_C U_W}{2(U_C + 2U_W)} \sum_{\bar{\omega}_n} (\tilde{\phi}_1 - \tilde{\phi}_4 - \frac{\tilde{V}_G}{U_W})^2. \end{aligned} \tag{25}$$

In this limit, the full action can be rewritten in terms of a "current" field $\chi(\tau)$ and a "charge" field $n(\tau)$ (and their Fourier transforms $\tilde{\chi}$ and $\tilde{n}$) defined as

$$\chi(\tau) = \frac{\phi_1 + \phi_4}{2} + \frac{k_F L}{2\sqrt{\pi}}, \quad \text{and} \quad n(\tau) = \frac{\phi_4 - \phi_1}{\sqrt{\pi}} + \frac{k_F L}{\pi} \ . \tag{26}$$

The action is given by

$$\begin{aligned} S_{eff,low} &= S_0 + S_{barrier} + S_{gate} \\ &= \frac{1}{2K_L} \sum_{\bar{\omega}_n} |\bar{\omega}_n| [(\tilde{\chi} - \frac{k_F L}{2\sqrt{\pi}})^2 + \frac{\pi}{4}(\tilde{n} - \frac{k_F L}{\pi})^2] \\ &\quad + \int d\tau [\frac{U_{eff}}{2}(n - n_0)^2 + V_1 \Lambda \cos(2\sqrt{\pi}\chi)\cos(\pi n)] \ , \end{aligned} \tag{27}$$

where $n_0 = (2k_C d + k_W l)/\pi - V_G/(\pi^{3/2} U_W)$ and $U_{eff} = \pi U_C U_W/(U_C + 2U_W)$. The derivation of the effective action in this limit follows the method outlined in Ref. [14]; however, their derivation was for a uniform wire with a single interaction parameter K, whereas we have three interaction parameters here. K_W acts only within the quantum wire delimited by the two contact regions, K_C acts within the contact region, and $K_L = 1$ outside the contact and wire region. The current field is interpreted as the number of particles transferred across the two barriers, and the charge field is the number of particles between the barriers. In the low frequency limit, the two barriers are clearly being seen as one coherent object with charge and current degrees of freedom. Since in the limit of weak barriers, $V_1 \ll U_{eff}$, the action is minimized when $n = n_0$, we can integrate out the quadratic fluctuations of $n - n_0$ to obtain an effective action only in terms of the single variable χ; we obtain

$$S_{low} = \int d\tau \ [\ 2V_1 \Lambda \cos(2\sqrt{\pi}\chi)\cos(\pi n_0) - \frac{2(V_1\Lambda)^2}{U_{eff}} (\pi \cos(2\sqrt{\pi}\chi)\sin(\pi n_0))^2 + \cdots \ ] \ . \tag{28}$$

The first term in this effective action is precisely the same term that is obtained for the impurity potential for a single barrier in terms of the variable χ.

In the low frequency limit, from Eq. (27), we see that the effective action contains extra terms due to the interference between the two barriers. It is easy to check that this effective action is invariant under $\chi \to \chi + \sqrt{\pi}, n \to n$; this is the same symmetry which exists for a single barrier [14], and it corresponds to the transfer of a single electron across the two barriers, and hence in our model, from the left lead to the right lead. But when n_0 is precisely equal to a half-odd-integer, the action is also invariant under $\chi \to \chi + \sqrt{\pi}/2, n \to 2n_0 - n$. As explained in Ref. [14], this corresponds to the 'transfer of half an electron across the wire' accompanied by a change in the charge state of the wire. In

the language of scattering, this corresponds to resonant tunneling through a virtual state. Within the TLL theory, this is the explanation of the Coulomb blockade phenomenon, which leads to steps or plateaus in the current versus gate voltage for quantum dots.

3.2 The case of spinful electrons

The spinless electron model is expected to be valid for real systems in the presence of strong magnetic fields which completely polarizes all the electrons in a given channel. However, for a real system without magnetic field, or in the presence of weak magnetic fields which do not polarize all the electrons, one has to study a model of electrons with spin. We shall study such a model here. Its modification due to the presence of a magnetic field will be studied in Sec. 5. The basic action of the model is a straightforward extension of the model for spinless fermions given in Eqs. (12) and (13), with $\phi_\uparrow$ denoting the spin up boson and $\phi_\downarrow$ denoting the spin down boson. However, since the Coulomb interaction couples the spin up and spin down fermions (for instance, remember the Hubbard term which is $U\sum_i n_{i\uparrow}n_{i\downarrow}$), the Luttinger model is diagonal only in terms of the charge and spin fields $\phi_\rho = (\phi_\uparrow + \phi_\downarrow)/\sqrt{2}$ and $\phi_\sigma = (\phi_\uparrow - \phi_\downarrow)/\sqrt{2}$. In terms of these fields S_0 is given by

$$S_0 = \int dt\ [\int_{-\infty}^{0} dx\mathcal{L}_1 + \int_0^d dx\mathcal{L}_2 + \int_d^{l+d} dx\mathcal{L}_3 + \int_{l+d}^{l+2d} dx\mathcal{L}_2 + \int_{l+2d}^{\infty} dx\mathcal{L}_1]\ , \qquad (29)$$

where

$$\begin{aligned} \mathcal{L}_1 &= \mathcal{L}(\phi_\rho; K_{L\rho}, v_L)\ +\ \mathcal{L}(\phi_\sigma; K_{L\sigma}, v_L)\ , \\ \mathcal{L}_2 &= \mathcal{L}(\phi_\rho; K_{C\rho}, v_{C\rho})\ +\ \mathcal{L}(\phi_\sigma; K_{C\sigma}, v_{C\sigma})\ , \\ \mathcal{L}_3 &= \mathcal{L}(\phi_\rho; K_{W\rho}, v_{W\rho})\ +\ \mathcal{L}(\phi_\sigma; K_{W\sigma}, v_{W\sigma})\ , \end{aligned} \qquad (30)$$

with $\mathcal{L}$ defined as before, $\mathcal{L}(\phi; K, v) = (1/2Kv)(\partial_\tau\phi)^2 + (v/2K)(\partial_x\phi)^2$, $K_{L\rho} = K_{L\sigma} = 1$ are the interaction parameters in the two external leads, and $K_{C/W\rho}$ and $K_{C/W\sigma}$ are the interaction parameters in the contacts and wire respectively. As for the spinless case, we include junction barrier terms of the form

$$S_{barrier} = \int d\tau \sum_{i=\downarrow,\uparrow} V_i\Lambda\ [\cos(2\sqrt{\pi}\phi_i(0,\tau)) + \cos(2\sqrt{\pi}\phi_i(L,\tau) + 2k_F L)], \qquad (31)$$

at the junctions of the contacts and the leads, and we assume that the barriers at the junctions of the wire and the contact are weak and can be ignored. The barrier action can be re-expressed in terms of the diagonal fields of the model (using $V_\uparrow = V_\downarrow = V$) as

$$S_{barrier} = V\Lambda \int d\tau[\cos(\sqrt{2\pi}\phi_{1\rho})\cos(\sqrt{2\pi}\phi_{1\sigma}) + \cos(\sqrt{2\pi}\phi_{4\rho} + 2k_F L)\cos(\sqrt{2\pi}\phi_{4\sigma})]\ , \qquad (32)$$

where, as before, we define $\phi_\rho(0) = \phi_{1\rho}$ and $\phi_\rho(L) = \phi_{4\rho}$ and similarly for the ϕ_σ fields. The gate voltage only couples to the charge degree of freedom within the wire region as

$$S_{gate} = \frac{V_G}{\sqrt{\pi}} \int d\tau(\phi_{3\rho} - \phi_{2\rho}) \ , \tag{33}$$

where $\phi_\rho(d) = \phi_{2\rho}$ and $\phi_\rho(l+d) = \phi_{3\rho}$ as before. So just as in the spinless case, we can integrate out all degrees of freedom except at $x = 0, d, l$ and L and obtain the effective action. The full details of the effective action are spelt out in Appendix B. By taking its high, intermediate and low frequency limits, we will be able to obtain conductance corrections just as we did for the spinless fermions.

In the high frequency limit where $\omega \gg v_{Ca}/d$ and v_{Wa}/l, the two barriers are seen as decoupled barriers, with

$$\begin{aligned} &S_{0,eff,high}(\phi_{1,\rho/\sigma}, \phi_{2,\rho/\sigma}, \phi_{3,\rho/\sigma}, \phi_{4,\rho/\sigma}) \\ &= \sum_{\bar{\omega}_n} |\bar{\omega}_n| [\frac{K_{L\rho} + K_{C\rho}}{2K_{L\rho}K_{C\rho}} (\tilde{\phi}^2_{1\rho} + \tilde{\phi}^2_{4\rho}) + \frac{K_{C\rho} + K_{W\rho}}{2K_{C\rho}K_{W\rho}} (\tilde{\phi}^2_{2\rho} \ + \ \tilde{\phi}^2_{3\rho}) \\ &\qquad + \quad \text{similar terms with } \rho \to \sigma]. \end{aligned} \tag{34}$$

The fields ϕ_{2a} and ϕ_{3a} are completely decoupled from the fields at $x = 0$ and L and can be integrated out yielding

$$\begin{aligned} &S_{0,eff,high}(\phi_{1,\rho/\sigma}, \phi_{4,\rho/\sigma}) \\ &= \frac{K_{L\rho} + K_{C\rho}}{2K_{L\rho}K_{C\rho}} \sum_{\bar{\omega}_n} |\bar{\omega}_n| (\tilde{\phi}^2_{1\rho} + \tilde{\phi}^2_{4\rho}) + \frac{K_{L\sigma} + K_{C\sigma}}{2K_{L\sigma}K_{C\sigma}} \sum_{\bar{\omega}_n} |\bar{\omega}_n| (\tilde{\phi}^2_{1\sigma} + \tilde{\phi}^2_{4\sigma}). \end{aligned} \tag{35}$$

Just as for the spinless case, we see that the parameters of the wire do not enter $K_{eff,\rho/\sigma} = K_{L\rho/\sigma}K_{C\rho/\sigma}/(K_{L\rho/\sigma} + K_{C\rho/\sigma})$. Nor does the gate voltage affect the action.

Just as in the spinless case, we have two possibilities for the intermediate frequency regime, the QW limit or the QPC limit.

For the QW limit, we have $v_W/l \ll \bar{\omega}_n \ll v_C/d$, and we obtain

$$\begin{aligned} &S_{eff,int}(\tilde{\phi}_{1,\rho/\sigma}, \tilde{\phi}_{2,\rho/\sigma}, \tilde{\phi}_{3,\rho/\sigma}, \tilde{\phi}_{4,\rho/\sigma}) \\ &= \frac{1}{2K_{L\rho}} \sum_{\bar{\omega}_n} |\bar{\omega}_n| (\tilde{\phi}^2_{1\rho} + \tilde{\phi}^2_{4\rho}) + \frac{1}{2K_{L\sigma}} \sum_{\bar{\omega}_n} |\bar{\omega}_n| (\tilde{\phi}^2_{1\sigma} + \tilde{\phi}^2_{4\sigma}) \\ &+ \frac{1}{2K_{W\rho}} \sum_{\bar{\omega}_n} |\bar{\omega}_n| (\tilde{\phi}^2_{2\rho} + \tilde{\phi}^2_{3\rho}) + \frac{1}{2K_{W\sigma}} \sum_{\bar{\omega}_n} |\bar{\omega}_n| (\tilde{\phi}^2_{2\sigma} + \tilde{\phi}^2_{3\sigma}) \\ &+ \frac{U_{C\rho}}{2} \sum_{\bar{\omega}_n} [(\tilde{\phi}_{1\rho} - \tilde{\phi}_{2\rho})^2 + (\tilde{\phi}_{3\rho} - \tilde{\phi}_{4\rho})^2] \end{aligned}$$

$$+\frac{U_{C\sigma}}{2}\sum_{\bar{\omega}_n}[(\tilde{\phi}_{1\sigma}-\tilde{\phi}_{2\sigma})^2+(\tilde{\phi}_{3\sigma}-\tilde{\phi}_{4\sigma})^2]+S_{gate}, \tag{36}$$

where $U_{C\rho,\sigma}=v_{C\rho,\sigma}/(K_{C\rho,\sigma}d)$ is the charging energy for the charge degrees of freedom. As the action is quadratic, we can integrate out the $\tilde{\phi}_{2,\rho/\sigma}$ and $\tilde{\phi}_{3,\rho/\sigma}$ spin and charge fields to be left with an action dependent only on the $\tilde{\phi}_{1,\rho/\sigma}$ and $\tilde{\phi}_{4,\rho/\sigma}$ spin and charge fields as given by

$$\begin{aligned}S_{0,eff,int}(\phi_{1,\rho/\sigma},\phi_{4,\rho/\sigma})= &\ \frac{K_{L\rho}+K_{W\rho}}{2K_{L\rho}K_{W\rho}}\sum_{\bar{\omega}_n}|\bar{\omega}_n|(\tilde{\phi}_{1\rho}^2+\tilde{\phi}_{4\rho}^2)\\ &+\frac{K_{L\sigma}+K_{W\sigma}}{2K_{L\sigma}K_{W\sigma}}\sum_{\bar{\omega}_n}|\bar{\omega}_n|(\tilde{\phi}_{1\sigma}^2+\tilde{\phi}_{4\sigma}^2)+\int d\tau\tilde{V}_G(\phi_{4\rho}-\phi_{1\rho}),\end{aligned} \tag{37}$$

where we have approximated $U_C+\bar{\omega}_n/(K_{W,\rho/\sigma})$ by U_C; this is justified in the intermediate regime as $T\ll v_{C,\rho/\sigma}/d$ and $K_{C,\rho/\sigma}\sim K_{W,\rho/\sigma}$.

In the QPC limit, we have

$$\begin{aligned}&S_{eff,int}(\tilde{\phi}_{1,\rho/\sigma},\tilde{\phi}_{2,\rho/\sigma},\tilde{\phi}_{3,\rho/\sigma},\tilde{\phi}_{4,\rho/\sigma})\\ &=\frac{1}{2K_{L\rho}}\sum_{\bar{\omega}_n}|\bar{\omega}_n|(\tilde{\phi}_{1\rho}^2+\tilde{\phi}_{4\rho}^2)+\frac{1}{2K_{L\sigma}}\sum_{\bar{\omega}_n}|\bar{\omega}_n|(\tilde{\phi}_{1\sigma}^2+\tilde{\phi}_{4\sigma}^2)\\ &+\frac{1}{2K_{C\rho}}\sum_{\bar{\omega}_n}|\bar{\omega}_n|(\tilde{\phi}_{1\rho}^2+\tilde{\phi}_{2\rho}^2+\tilde{\phi}_{3\rho}^2+\tilde{\phi}_{4\rho}^2)+\frac{1}{2K_{C\sigma}}\sum_{\bar{\omega}_n}|\bar{\omega}_n|(\tilde{\phi}_{1\sigma}^2+\tilde{\phi}_{2\sigma}^2+\tilde{\phi}_{3\sigma}^2+\tilde{\phi}_{4\sigma}^2)\\ &+\frac{U_{W\rho}}{2}\sum_{\bar{\omega}_n}(\tilde{\phi}_{2\rho}-\tilde{\phi}_{3\rho})^2+S_{gate},\end{aligned} \tag{38}$$

where $U_{W\rho}=v_{W\rho}/(K_{W\rho}l)$ is the charging energy for the charge degrees of freedom in the wire. As before, we may integrate out the inner degrees of freedom to find that

$$S_{0,eff,int}(\tilde{\phi}_{1,\rho/\sigma},\tilde{\phi}_{4,\rho/\sigma}) \ = \ S_{0,eff,high}(\tilde{\phi}_{1,\rho/\sigma},\tilde{\phi}_{4,\rho/\sigma}) \tag{39}$$

as expected.

Finally, in the low frequency limit $\bar{\omega}_n\ll v_C/d$ and v_W/l, as in the spinless case, the terms multiplying $1/K_{C\rho/\sigma}$ and $1/K_{W\rho/\sigma}$ in Eq. (144) in Appendix B become constant 'mass' terms. We get the full effective action as

$$\begin{aligned}&S_{eff,low}(\phi_{1,\rho/\sigma},\phi_{2,\rho/\sigma},\phi_{3,\rho/\sigma},\phi_{4,\rho/\sigma})\\ &=\frac{1}{2K_{L\rho}}\sum_{\bar{\omega}_n}|\bar{\omega}_n|(\tilde{\phi}_{1\rho}^2+\tilde{\phi}_{4\rho}^2)+\int d\tau[\frac{v_{C\rho}}{K_{C\rho}d}\{(\phi_{1\rho}-\phi_{2\rho})^2+(\phi_{3\rho}-\phi_{4\rho})^2\}\end{aligned}$$

$$+ \frac{v_{W\rho}}{K_{W\rho}}(\phi_{2\rho} - \phi_{3\rho})^2 + \text{similar terms with } \rho \to \sigma] + \frac{eV_G}{\sqrt{\pi}} \int d\tau [\phi_{3\rho} - \phi_{2\rho}]$$
$$+ V\Lambda \int d\tau [\cos(\sqrt{2\pi}\phi_{1\rho}) \cos(\sqrt{2\pi}\phi_{1\sigma}) + \cos(\sqrt{2\pi}\phi_{4\rho} + 2k_F L) \cos(\sqrt{2\pi}\phi_{4\sigma})] \ . \tag{40}$$

Just as we did in the spinless case, we now integrate out the fields at $x = d$ and $l + d$, in terms of which the above action is quadratic, to get

$$\begin{aligned} & S_{eff,low}(\phi_{1,\rho/\sigma}, \phi_{4,\rho/\sigma}) \\ & = \frac{1}{2K_{L\rho}} \sum_{\bar{\omega}_n} |\bar{\omega}_n| (\tilde{\phi}_{1\rho}^2 + \tilde{\phi}_{4\rho}^2) + \frac{U_{C\rho} U_{W\rho}}{2(U_{C\rho} + 2U_W \rho)} \sum_{\bar{\omega}_n} (\tilde{\phi}_{1\rho} - \tilde{\phi}_{4\rho} - \frac{\tilde{V}_G}{U_{W\rho}})^2 \\ & \quad + \frac{1}{2K_{L\sigma}} \sum_{\bar{\omega}_n} |\bar{\omega}_n| (\tilde{\phi}_{1\sigma}^2 + \tilde{\phi}_{4\sigma}^2) + \frac{U_{C\sigma} U_{W\sigma}}{2(U_{C\sigma} + 2U_W \sigma)} \sum_{\bar{\omega}_n} (\tilde{\phi}_{1\sigma} - \tilde{\phi}_{4\sigma})^2. \end{aligned} \tag{41}$$

Here, we see that the effective mass terms are given by $U_{eff,\rho} = \pi U_{C\rho} U_{W\rho}/(U_{C\rho} + 2U_W \rho)$ and $U_{eff,\sigma} = \pi U_{C\sigma} U_{W\sigma}/(U_{C\sigma} + 2U_{W\sigma})$ for the 'charge' and 'spin charge' fluctuations respectively. We denote the 'charge on the quantum wire' fields as $n_\rho = \sqrt{2/\pi}(\phi_{1\rho} - \phi_{4\rho})$ and $n_\sigma = \sqrt{2/\pi}(\phi_{1\sigma} - \phi_{4\sigma})$ respectively, and the 'current' fields as $\chi_\rho = (\phi_{1\rho} + \phi_{4\rho})/\sqrt{2}, \chi_\sigma = (\phi_{1\sigma} + \phi_{4\sigma})/\sqrt{2}$ along with their appropriate Fourier transforms $\tilde{\chi}_{\rho/\sigma}$ and $\tilde{n}_{\rho/\sigma}$ just as we did in the spinless case. The action then takes the following form,

$$\begin{aligned} S_{eff,low} \ = \ & \frac{1}{2K_{L\rho}} \sum_{\bar{\omega}_n} |\bar{\omega}_n| [|\tilde{\chi}_\rho - \frac{k_F d}{\sqrt{\pi}}|^2 + \frac{\pi}{4} |\tilde{n}_\rho - \frac{2k_F d}{\pi}|^2] + \int d\tau \frac{U_{eff,\rho}}{2} (n_\rho - n_{0\rho})^2 \\ & + \frac{1}{2K_{L\sigma}} \sum_{\bar{\omega}_n} |\bar{\omega}_n| [|\tilde{\chi}_\sigma|^2 + \frac{\pi}{4} |\tilde{n}_\sigma|^2] + \int d\tau \frac{U_{eff,\sigma}}{2} (n_\sigma)^2 \\ & + 2V\Lambda \int d\tau [\cos(\sqrt{\pi}\chi_\rho) \cos(\frac{\pi n_\rho}{2}) \cos(\sqrt{\pi}\chi_\sigma) \cos(\frac{\pi n_\sigma}{2}) \\ & \qquad + \sin(\sqrt{\pi}\chi_\rho) \sin(\frac{\pi n_\rho}{2}) \sin(\sqrt{\pi}\chi_\sigma) \sin(\frac{\pi n_\sigma}{2})] \ . \end{aligned} \tag{42}$$

We have used the fact that since it is only the ρ field which couples to the gate voltage and not the σ fields, we only get $n_{0\rho} = (2k_C d + k_W l)/\pi - V_G/(\pi^{3/2} U_{W\rho})$ and $n_{0\sigma} = 0$.

We now study the symmetries of the effective action to find out the possible resonances. As in the spinless fermion case, this effective action is invariant under the transformation $\chi_\rho \to \chi_\rho + \sqrt{\pi}$ and $\chi_\sigma \to \chi_\sigma + \sqrt{\pi}$, which corresponds to the transfer of either an up electron or a down electron through the two barriers. But besides this symmetry, there are also some special gate voltages at which one can get resonance symmetries. This can

happen when we adjust the gate voltage so as to make $n_{0\rho}$ an odd integer. In that case, V_{eff} is invariant under

$$\begin{aligned} &n_\sigma \to -n_\sigma, \quad n_\rho \to 2n_{0\rho} - n_\rho \ \text{ in conjunction with} \\ &\text{either } \ (i)\ \chi_\rho \to \chi_\rho + \sqrt{\pi}, \quad \chi_\sigma \to \chi_\sigma \ \text{ or } \ (ii)\ \chi_\sigma \to \chi_\sigma + \sqrt{\pi}, \quad \chi_\rho \to \chi_\rho \ . \end{aligned} \tag{43}$$

As explained in Ref. [14], this resonance which occurs when $n_{0\rho}$ is tuned to be an odd integer, is called a Kondo resonance because it happens when two spin states in the island with $n_\sigma = \pm 1$ become degenerate.

The kind of resonance which was seen for spinless fermions when two charge states on the island becomes degenerate is harder to see for spinful fermions. Two charge states become degenerate when $n_{0\rho}$ is tuned to be a half-odd-integer. But, in that case, the effective action in Eq. (42) does not have any extra 'resonance symmetry' unless $n_{0\sigma}$ (which we have set to be zero) is also tuned to be a half-odd-integer. But non-zero $n_{0\sigma}$ is only possible when there is an effective magnetic field or $SU(2)$ breaking field just over the quantum wire. This is because the Zeeman term is given by the Hamiltonian density

$$\mathcal{H}_{Zeeman} = -h(\partial_x \phi_\uparrow - \partial_x \phi_\downarrow) = -\sqrt{2} h \partial_x \phi_\sigma \ , \tag{44}$$

and it does not lead to any boundary terms as long as the magnetic field is felt through the full sample. However, although in current experiments it is not possible to tune the $SU(2)$ breaking to occur only between the two barriers, it could be possible in future experiments. Hence it is of interest to look for possible resonances in this case as well. We see that if one could arrange to tune both the gate voltage and the magnetic field (adjusted to be just over the quantum wire) so that $n_{0\rho}$ and $n_{0\sigma}$ are both half-odd-integers, the effective action in Eq. (42) is symmetric under $n_\rho \to 2n_{0\rho} - n_\rho$, $n_\sigma \to 2n_{0\sigma} - n_\sigma$, $\chi_\rho \to \chi_\rho + \sqrt{\pi}/2$, and $\chi_\sigma \to \chi_\sigma + \sqrt{\pi}/2$. This resonance is exactly analogous to the resonance that existed for spinless fermions and corresponds to hopping an electron from either of the leads to the wire. But since this requires the tuning of two parameters, it is a 'higher' order resonance and will be more difficult to achieve experimentally.

In fact, if we allow for non-zero $n_{0\sigma}$, then the effective action also has the symmetry

$$\begin{aligned} &n_\rho \to -n_\rho, \quad n_\sigma \to 2n_{0\sigma} - n_\sigma \ \text{ in conjunction with} \\ &\text{either } \ (i)\ \chi_\rho \to \chi_\rho + \sqrt{\pi}, \quad \chi_\sigma \to \chi_\sigma \ \text{or} \quad (ii)\ \chi_\sigma \to \chi_\sigma + \sqrt{\pi}, \quad \chi_\rho \to \chi_\rho \ , \end{aligned} \tag{45}$$

when $n_{0\sigma}$ is an odd integer and $n_{0\rho} = 0$. But this is hard to achieve, because one needs to tune the external gate voltage so as to cancel the field due to the presence of all the other electrons within the two barriers as well. Hence, this resonance will not be easy to see in experiments. Moreover, it will show up in the spin conductance and not the charge conductance.

In conclusion, we have studied in this section the effective actions of our model for both spinless and spinful fermions, and used them to obtain conductance corrections away from resonances (where the conduction is perfect) as a function of finite temperature and finite length of the wire. The same technique will again be used in Sec. 5, where it will be used to study the symmetries and obtain the conductance corrections of the quantum wire in the presence of a magnetic field.

4 Computation of the conductances

In this section, we compute the conductances of our TLL quantum wire with contacts, two semi-infinite Fermi liquid leads and two weak barriers at the junctions of the contacts and the leads, for both spinless and spinful electrons, perturbatively in the barrier strength. We explicitly derive an expression for the conductance to lowest order in barrier strength (quadratic) in terms of the Green's functions of the model. The RG flow of the barrier strengths has been incorporated through a function $\chi(x, y)$. Thus, the behavior of the Green's functions in the different frequency regimes determines the conductance corrections. The conductance corrections for a simpler version of the model of the quantum wire (i.e., one in which the quantum wire is directly connected to the Fermi leads through two weak junction barriers) has already been studied by Safi and Schulz [24], who used a real time formulation and computed time-dependent Green's functions. The perturbative corrections in the Kane-Fisher imaginary time formalism was also extended to the case of finite length wires by Maslov [27] and Furusaki and Nagaosa [18], who computed frequency dependent Green's functions. For our model, with five distinct spatial regions with their boundaries, the real time picture of TLL quasiparticle waves reflecting back and forth between the boundaries (as developed by Safi and Schulz [16]) is more cumbersome; hence, we use the imaginary time formulation and compute frequency dependent Green's functions.

4.1 The formulation of the conductance expressions

The current through a clean quantum wire through which spinless electrons are traveling can be found using the Kubo formula

$$j(x) = \lim_{\omega \to 0} \int dy \sigma(x, y, \omega) E(y, \omega) \ , \tag{46}$$

where $\sigma(x, y, \omega)$ is the non-local conductivity and is related to the two-point Green's function $G(x, y, \omega)$ at finite frequency ω as

$$\sigma(x, y, \omega) = \ -i\frac{2\omega e^2}{h} G(x, y, \omega) \ . \tag{47}$$

For our model of the quantum wire, $G_{\bar{\omega}}(x, y)$ has been computed in Appendix D. Note that the real frequency ω is related to $\bar{\omega}$ (used in the earlier sections) by the analytic continuation $\omega = i\bar{\omega} + \epsilon$. From Appendix D, we find that $G_{\bar{\omega}}(x, y) = K_L/(2|\bar{\omega}|)$ + non-singular terms in $\bar{\omega}$ in the limit $\omega \to 0$ for our model. hence the dc conductance g_0 is given by

$$g_0 = \lim_{\omega \to 0} \sigma(x, y, \omega) = \frac{e^2}{h} \ . \tag{48}$$

This shows perfect dc conductance through the system as in the earlier models without contacts[16, 17]. This result remains unchanged for the case of electrons with spin, except for a multiplication of the conductance by a factor of two.

For a quantum wire in the presence of stationary impurities, an explicit expression for the conductance can be derived to lowest (quadratic) order in the impurity strength from the partition function, using perturbation theory [14, 24, 27]. The renormalization group (RG) equations for the barriers (discussed in detail in subsection 4.4) imply that the barrier strengths grow under renormalization. However, it is only for very low temperatures or very long wire lengths that there will be considerable renormalization. In real experimental setups, the length of the wire is in the range of micrometers and the temperatures in the range of a Kelvin; hence one does not expect much renormalization. Hence, it is expected that the barrier strengths remain small enough for perturbation theory to be applicable. We follow the methods of Safi and Schulz [24] and Maslov [27], who derived explicitly a conductance expression for a non-translationally invariant system and obtained

$$g = g_0 K_L (1 - \mathcal{R}) \ , \tag{49}$$

where R is the perturbative correction to second order in the impurity strength. $\mathcal{R}$ is given by

$$\mathcal{R} = g_0 K_L \sum_{m=1}^{\infty} m^2 c_m^2 \mathcal{R}^{(m)} \ , \tag{50}$$

where the c_m's are the coefficients for the terms in the Haldane representation of the fermionic density, and $\mathcal{R}^{(m)}$ is the correction due to the back-scattering of m electrons given by

$$\mathcal{R}^{(m)} = \int\int dx dy V(x) V(y) \cos[2m(\xi(x) - \xi(y))] \chi_m(x, y) \ . \tag{51}$$

In the above expression, $V(x)$ is the bare potential of the impurities, ξ is a phase factor which includes the $k_F x$ factor coming from the back-scattering process and other factors which arise due to the removal of the forward scattering terms from the Hamiltonian by shifts in the bosonic field ϕ, and $\chi_m(x,y)$ is a factor which incorporates the renormalization group (RG) flows of the barrier strengths. In general, it is given by a two-point correlation function defined as

$$\chi_m(x,y) = \frac{1}{T^2} e^{-2m^2 G_0(x,x,\tau_0) - 2m^2 G_0(y,y,\tau_0)} \int_0^\infty dt e^{4m^2 G_0(x,y,it+\pi/2)} \ , \tag{52}$$

$G_0(x,y,it)$ is the two-point Green's function for a clean quantum wire. Here, the Green's functions are in terms of the imaginary time $\tau = it$. $\tau_0 \sim 1/\Lambda$ is the inverse of the high energy cutoff. In a later subsection, we show how the one-point function $\chi_m(x,x)$ can be obtained directly from the RG equation for the barriers.

For our system, we shall instead compute the two-point Green's function in terms of $\bar{\omega}$, in terms of which, the correction to the conductance is given by (specializing to the case $m = 1$)

$$\begin{aligned} R^{(1)} &= \lim_{\omega\to 0} \frac{\omega}{(g_0 K_L)^2} \int dx' \int dy' G_0(x,x',\omega) G_0(y,y',\omega) \cos[2(\xi(x') - \xi(y'))] \times \\ &\qquad V(x')V(y') Im(F(x',y',\omega) - F(x',y',0)) \\ &= \int dx' \int dy' \cos[2(\xi(x') - \xi(y'))] V(x')V(y') \lim_{\omega\to 0} \frac{dF(x',y',\omega)}{d\omega}, \end{aligned} \tag{53}$$

where

$$\begin{aligned} &F(x',y',\omega) \\ &= \int_{-\infty}^{\infty} dt e^{i\omega t} \exp(-2\pi \sum_{\bar{\omega}'_n} [G_0(x',x',\bar{\omega}'_n) + G_0(y',y',\bar{\omega}'_n) - 2G_0(x',y',\bar{\omega}'_n)\cos(\bar{\omega}'_n \tau)]). \end{aligned} \tag{54}$$

Note that the Green's functions in the prefactors of $R^{(1)}$ are dependent on the external driving frequency, but the Green's functions in the exponential depend only on the Matsubara frequencies $\bar{\omega}'_n$, and not on the external driving frequency ω or its analytic continuation $\bar{\omega}$. The sum over the Matsubara frequencies are cutoff at the low energy end by $\bar{\omega}'_{n=1} \sim k_B T$ and at the upper end by the high energy cutoff Λ. In evaluating $R^{(1)}$, we will approximate $\sum_{\bar{\omega}'_n}$ by $\int d\bar{\omega}'/(2\pi)$ which is reasonable since we always assume that the temperature T is much smaller than the cutoff Λ.

4.2 Results for the Quantum Wire

We will concentrate here on calculating the conductance of a quantum wire system in which the length of the quantum wire l is much greater than the length of the contact

regions d. Also, we will finally be interested in studying the effects of the junction barriers placed at the two lead-contact junctions (as explained earlier). Hence, for our model

$$V(x) = V_1 \Lambda \delta(x) + V_2 \Lambda \delta(x - L). \tag{55}$$

For this potential, we can obtain the expression for the conductance corrections as

$$\begin{aligned} R^{(1)} &= \Lambda^2 \lim_{\omega \to 0} [V_1^2 Im \frac{dF(0,0,\omega)}{d\omega} + V_2^2 Im \frac{dF(L,L,\omega)}{d\omega} \\ &\quad + 2V_1 V_2 Im \frac{dF(0,L,\omega)}{d\omega} \cos(\xi(0) - \xi(L))]. \end{aligned} \tag{56}$$

- Spinless electrons

  Now, the expression for the one-point Green's function (in frequency space) for a barrier placed inside the contact region on the left of the QW and at a distance a from the left lead-contact junction (which is taken to be the origin, giving the hierarchy of length scales $a \ll d \ll l$) can be easily obtained from Appendix D. It is given by

$$G_{\bar{\omega}}(x = a, y = a) \simeq \frac{K}{2|\bar{\omega}|} \ , \tag{57}$$

  where

$$K = \begin{cases} K_C & \text{for } |\bar{\omega}| \gg v_C/a \\ \frac{2K_L K_C}{K_L + K_C} & \text{for } v_C/d \ll |\bar{\omega}| \ll v_C/a \\ \frac{2K_L K_W}{K_L + K_W} & \text{for } v_W/l \ll |\bar{\omega}| \ll v_C/d \\ K_L & \text{for } |\bar{\omega}| \ll v_W/l \ . \end{cases}$$

  For our model with a barrier at the left lead-contact junction, $a = 0$ and the first frequency regime does not exist.

  The two-point Green's function $G(x, y)$ for y in the left contact region and x anywhere is given in Appendix D. By setting $y = 0$ (i.e., at the first barrier) and $x = L = l + 2d$ (i.e., at the second barrier) we obtain the conductances in the different frequency regimes given by

$$\begin{aligned} G &= \frac{2K_C(1+\gamma_1)^2}{(2 + K_C/K_W + K_W/K_C)} \frac{\exp[-|\bar{\omega}|(\frac{2d}{v_C} + \frac{l}{v_W})]}{|\bar{\omega}|} \quad \text{for} \quad |\bar{\omega}| \gg v_W/l \gg v_C/d \\ &= \frac{2K_C(1+\gamma_1)^2}{(2 + K_C/K_W + K_W/K_C)} \frac{\exp[-|\bar{\omega}|(\frac{2d}{v_C})]}{|\bar{\omega}|} \quad \text{for} \quad v_W/l \gg |\bar{\omega}| \gg v_C/d \\ &= \frac{K_L}{2|\bar{\omega}|} \quad \text{for} \quad v_C/d, v_W/l \gg |\bar{\omega}|, \end{aligned} \tag{58}$$

where $\gamma_1 = \frac{K_L - K_C}{K_L + K_C}$. Thus, we see that $G(x, y, \bar{\omega}')$ decays exponentially to zero except at the lowest frequency regime where $G(x, y, \bar{\omega}') = G(x, x, \bar{\omega}') = G(y, y, \bar{\omega}')$.

To obtain the conductance corrections, we use the above Green's functions to compute $F(x', y', \bar{\omega}')$ in each of these frequency regimes. For the high frequency regime, it is simply given by

$$\begin{aligned} F(x', y', \omega) &= \int_{-\infty}^{\infty} dt e^{i\omega t} \exp[-2\pi \int_T^{\Lambda} \frac{d\bar{\omega}'}{2\pi} (\frac{K_{eff}}{|\bar{\omega}'|} - 2G(x', y', \bar{\omega}') \cos \bar{\omega}' \tau)] \\ &= \int_{-\infty}^{\infty} \frac{1}{T} dz e^{i\omega z/T} (\frac{T}{\Lambda})^{2K_{eff}} \exp[-2\pi \int_T^{\Lambda} \frac{d\bar{\omega}'}{2\pi} 2G(x', y', \bar{\omega}') \cos \bar{\omega}' \tau], \end{aligned} \tag{59}$$

where $K_{eff} = K_L K_C/(K_L + K_C)$, and in the second line, we have scaled t by T, i.e., we have used $t = z/T$ to write the integral in terms of dimensionless variables so that the temperature power-laws can be made explicit. When $x' \neq y'$, $G(x', y', \bar{\omega}') \to 0$, so that one can check that $lim_{\omega \to 0} Im \frac{dF}{d\omega}$ also tends to zero. This means that the cross-term in Eq. (56) does not contribute. For each of the terms involving just one barrier, we find that

$$lim_{\omega \to 0} Im \frac{dF}{d\omega} = \frac{1}{T^2} (\frac{T}{\Lambda})^{2K_{eff}} \exp[-\int_T^{\Lambda} d\bar{\omega}' \frac{K_{eff}}{|\bar{\omega}'|} \cos \bar{\omega}' \tau]. \tag{60}$$

Hence, we obtain the following answer for the conductance correction for high temperatures $T \gg T_d \equiv v_C/(k_B d)$,

$$g = g_0 K_L [1 - c_1 (\frac{T}{\Lambda})^{2(K_{eff} - 1)} (|V_1|^2 + |V_2|^2)], \tag{61}$$

where c_1 is a dimensionful constant dependent on factors like the contact quasiparticle velocity v_C, but is independent of the gate voltage V_G.

For intermediate temperatures where $T_l \equiv v_W/(k_B l) \ll T \ll T_d$ the calculation is very similar to that performed for the high frequency case, except that the integral over the Matsubara frequencies is now split into two regions

$$\begin{aligned} F(x', y', \omega) &= \int_{-\infty}^{\infty} dt e^{i\omega t} \exp[-2\pi (\int_T^{T_d} + \int_{T_d}^{\Lambda}) \frac{d\bar{\omega}'}{2\pi} \frac{K}{|\bar{\omega}'|}] \\ &\qquad \exp[2\pi \int_T^{\Lambda} \frac{d\bar{\omega}'}{2\pi} 2G(x', y', \bar{\omega}') \cos \bar{\omega}' \tau] \ . \end{aligned} \tag{62}$$

The rest of the calculations go through as above, and we find that the conductance expression is

$$g = g_0 K_L [1 - c_2 (\frac{T_d}{\Lambda})^{2(K_{eff} - 1)} (\frac{T}{T_d})^{2(\tilde{K}_{eff} - 1)} (|V_1|^2 + |V_2|^2)], \tag{63}$$

where $\tilde{K}_{eff} = K_L K_W/(K_L + K_W)$ and c_2 is a dimensionful constant which is dependent on V_G.

Finally, for very low temperatures $T \ll T_l$, the sum over Matsubara frequencies split into three regions so that we have

$$F(x',y',\omega) = \int_{-\infty}^{\infty} dt e^{i\omega t} \exp[-2\pi(\int_{T}^{T_l} + \int_{T_l}^{T_d} + \int_{T_d}^{\Lambda})\frac{d\bar{\omega}'}{2\pi}\frac{K}{|\bar{\omega}'|}] \exp[2\pi \int_{T}^{\Lambda} \frac{d\bar{\omega}'}{2\pi} 2G(x',y',\bar{\omega}')\cos\bar{\omega}'\tau] \ . \quad (64)$$

Furthermore, in this regime, the cross-term does not vanish; in fact, for $x' \neq y'$, we have $G(x',y',\bar{\omega}) = G(x',x',\bar{\omega}) = G(y',y',\bar{\omega})$, so that $F(x',y',\omega) = F(x',x',\omega) = F(y',y',\omega)$. The contribution of the cross term is hence identical to that of the terms due to a single barrier. Hence, we obtain the corrections to the conductance as

$$g = g_0 K_L[1 - c_3(\frac{T}{T_l})^{2(K_L-1)}(\frac{T_d}{\Lambda})^{2(K_{eff}-1)}(\frac{T_l}{T_d})^{2(\tilde{K}_{eff}-1)}|V_1+V_2|^2] \ , \quad (65)$$

where c_3 is a dimensionful constant similar in nature to c_2; thus the two barriers are seen coherently.

Note that the power-laws come purely from the one-point Green's functions, whereas the phase coherence between the barriers is determined by the behavior of the two-point correlation function. At high or intermediate frequencies, $lim_{\omega\to 0} Im\frac{dF(x',y',\omega)}{d\omega}$ tends to zero for $x' \neq y'$ leading to the lack of phase coherence between the two barriers. At very high temperatures, the interaction parameters of the contact region K_C and the lead region K_L controls the renormalization of a barrier in the contact region. As the temperature is lowered, the phase coherence length of the electronic excitations increases, and the renormalization exponent makes a crossover to a combination of the interaction parameters of the contact and QW, and finally to that of the lead alone at the lowest temperature regime. The lowest temperature regime is also the one in which resonant transport through both the lead-contact junction barriers can take place as phase coherence over the entire system is achieved at these temperatures.

- Electrons with spin

  The above expressions were given for a model of the QW system but for spinless electrons. Let us now see what the conductance expressions are for electrons with spin. These expressions can be derived in the same way as for spinless electrons by using the appropriate Green's functions for spin and charge fields. This gives us for

the high temperature regime of $T_d \ll T$

$$g = 2g_0 K_L[1 - c_4(\frac{T}{\Lambda})^{2(K_{eff}-1)}(|V(0)|^2 + |V(l+2d)|^2)], \tag{66}$$

where now $K_{eff} = K_L K_{C\rho}/(K_L + K_{C\rho}) + K_L K_{C\sigma}/(K_L + K_{C\sigma})$, and c_4 is a dimensionful constant much like c_1 for the spinless case (i.e., dependent on the contact charge velocity $v_{C,\rho}$ but independent of the gate voltage V_G). For the intermediate temperature range $T_l \ll T \ll T_d$, we find

$$g = 2g_0 K_L[1 - c_5(\frac{T_d}{\Lambda})^{2(K_{eff}-1)}(\frac{T}{T_d})^{2(\tilde{K}_{eff}-1)}(|V(0)|^2 + |V(l+2d)|^2)] \ , \tag{67}$$

where $\tilde{K}_{eff} = K_L K_{W\rho}/(K_L + K_{W\rho}) + K_L K_{W\sigma}/(K_L + K_{W\sigma})$, and c_5 is a constant similar to c_2 for the spinless case (i.e., dependent on V_G). Finally, for the low temperature regime $T \ll T_l$, we obtain

$$g = 2g_0 K_L[1 - c_6(\frac{T}{T_l})^{2(K_L-1)}(\frac{T_d}{\Lambda})^{2(K_{eff}-1)}(\frac{T_l}{T_d})^{2(\tilde{K}_{eff}-1)}|V(0) + V(l+2d)|^2] \ , \tag{68}$$

where c_6 is similar in nature to c_3 for the spinless case.

4.3 Results for the Quantum Point Contact

The Quantum Point Contact (QPC) is simply a quantum wire system in which the length of the quantum wire region $l \sim 0.2 - 0.5\mu m$ (i.e., the region undergoing the constriction due to the application of the gate voltage) is much reduced in comparison to typical lengths for a quantum wire $l \sim 2 - 20\mu m$. Thus, in our model of the quantum wire system, we can reach the QPC by studying the limit when the contact region length d is much greater than the wire length l. Let us then study the effects of barriers/impurities placed in the contact and wire region of the QPC.

- Spinless electrons

  In order to study the effect of a weak barrier placed in the contact region such that its distance a from the left lead-contact junction falls in the hierarchy of $a \ll l \ll d$, we again start by computing the one-point Green's function for such an impurity. We find that

$$G_{\bar{\omega}}(x = a, y = a) \simeq \frac{K}{2|\bar{\omega}|}, \tag{69}$$

where

$$K = \begin{cases} K_C & \text{for } |\bar{\omega}| \gg v_C/a \\ \frac{2K_L K_C}{K_L+K_C} & \text{for } v_W/l \ll |\bar{\omega}| \ll v_C/a \\ \frac{2K_L K_C}{K_L+K_C} & \text{for } v_C/d \ll |\bar{\omega}| \ll v_W/l \\ K_L & \text{for } |\bar{\omega}| \ll v_C/d \ . \end{cases}$$

As before, for the two-point function, we find that the high and low frequency limits are the same as that given in Eq. (58) for the QW, but for $T_d \ll T \ll T_l$, the answer turns out to be the same as in the high frequency limit. This is similar to what one sees for the one-point Green's functions above as well. So, without giving any further derivations, we directly quote the expressions for the conductance corrections. In the high and intermediate frequency regimes, the conductance is given by

$$g = g_0 K_L[1 - c_i(\frac{T}{\Lambda})^{2(K_{eff}-1)}(|V_1|^2 + |V_2|^2)], \tag{70}$$

where $i = 4, 5$ allows for the constant to be different in the high and intermediate frequency regimes. For the low frequency regime, we get

$$g = g_0 K_L[1 - c_6(\frac{T}{T_d})^{2(K_L-1)}(\frac{T_d}{\Lambda})^{2(K_{eff}-1)}(|V_1 + V_2|^2)], \tag{71}$$

It is clear from the above expressions that the contributions of barriers in the contacts of a QPC are always going to be independent of the gate voltage V_G as the QPC interaction parameter K_W does not enter anywhere. Thus, such an impurity would always lead to a flat and channel independent renormalized conductance. It should be noted that we have found from a similar calculation that even for an impurity placed deep inside the contact (i.e., with the hierarchy of $l \ll a \ll d$), the above conclusions still remain true; this is because the only change that takes place is that $K = K_C$ (rather than the combination of K_L and K_C found earlier) for the regime of $v_W/l \ll |\bar{\omega}| \ll v_C/a$.

Finally, let us study the effect of an impurity placed inside the QPC itself. We find the one-point Green's function for such a case (with the hierarchy of $l \ll d < a$) to be

$$G_{\bar{\omega}}(x = a, y = a) \simeq \frac{K}{2|\bar{\omega}|}, \tag{72}$$

where

$$K = \begin{cases} K_W & \text{for } |\bar{\omega}| \gg v_W/l \\ K_C & \text{for } v_C/d \ll |\bar{\omega}| \ll v_W/l \\ K_L & \text{for } |\bar{\omega}| \ll v_C/a \quad . \end{cases}$$

We have here only three frequency regimes as the regime of $v_C/d \ll |\bar{\omega}| \ll v_W/l$ cannot be taken sensibly within the given hierarchy of length scales. This shows again that the effect of an impurity placed within the QPC will always be dependent on the gate voltage V_G, and can never lead to flat and channel independent renormalizations of the conductance.

- Electrons with spin

  The generalization to spinful electrons can be obtained just as was done for quantum wires with the appropriate substitutions.

4.4 Evaluation of the conductances from the effective actions using the RG equations

Here, we note that the above results for the conductances could have been anticipated by computing the RG equation for the impurity potentials using the effective actions calculated in Sec. 3.

The conductance is governed by the renormalized barrier potentials at the two junctions. Since the interaction is repulsive, the barrier potentials are expected to grow as a function of the frequency cutoff. This is what leads to the result that any impurity potential, however small, eventually cuts the wire; in the zero temperature limit, there is no transmission at all [14]. However, at a finite temperature T, finite wire length l or finite contact length d, the growth is cutoff by either T, v_W/L or v_C/d. In fact, since the energy scales in the problem are the temperature k_BT, the high frequency cutoff Λ and those related to the contact length $k_BT_d = v_C/d$ and the wire length $k_BT_l = v_W/l$, we can see that there will exist two energy scale crossovers in the system — one from T/Λ to T/T_d and the other from T/T_d to T/T_l for $d \ll l$ (the QW limit), or from T/Λ to T/T_l and then from T/T_l to T/T_d for $l \ll d$ (the QPC limit).

In fact, an explicit RG calculation of either of the individual barrier strengths in the high, intermediate and low frequency regimes simply involves computing the dimension of $\cos(2\sqrt{\pi}\phi_1)$ or $\cos(2\sqrt{\pi}\phi_4)$ (which turn out to be the same) using those respective actions. For example, for the high frequency effective action given in Eq. (17), the RG equation

for a single barrier is given by

$$\frac{dV_1}{d\lambda} = (1 - \frac{2K_C K_L}{K_C + K_L})V_1 \equiv (1 - K_{eff})V_1 \ , \tag{73}$$

where $\lambda = \ln\frac{\Lambda(\lambda)}{\Lambda}$. Using this, we can get the renormalized barrier strength to be

$$V_1^{ren} = V_1(\frac{T}{\Lambda})^{K_{eff}-1} \tag{74}$$

in the high frequency regime $T \gg T_d$, where we have used T to cutoff the RG flow (which begins from Λ). From this, we infer that to quadratic order, the T dependence of the conductance corrections is given by

$$g = \frac{e^2}{h}[1 - \tilde{c}_1 V_1^2(\frac{T}{\Lambda})^{2(K_{eff}-1)}] \quad \text{for} \quad T \gg T_d \ , \tag{75}$$

where $\tilde{c}_1$ is a dimensionful constant like c_1 defined earlier containing factors like v_C but is, most importantly, independent of the gate voltage V_G. Comparing with Eq. (61), we see that if we include the subtraction due to two barriers, the expressions are identical.

In the intermediate regime of $T_l \ll T \ll T_d$, the RG equation for the same barrier now becomes

$$\frac{dV_1}{d\lambda} = (1 - \frac{2K_C K_W}{K_W + K_L})V_1 \equiv (1 - \tilde{K}_{eff})V_1 \ . \tag{76}$$

using the effective action in Eq. (21). At the same time, the appearance of the energy scale v_C/d (through U_C) in the effective action in this temperature regime and the taking of the approximation $\bar{\omega}_n \ll U_C$ means that v_C/d has replaced Λ as the high energy cutoff in the expression for the T dependence of the conductance correction. The influence of those degrees of freedom whose energies lie between v_C/d and Λ can be taken into account by noting that they will contribute a factor of $(T_d/\Lambda)^{2(K_{eff}-1)}$; this is because these degrees of freedom have been integrated away during the RG procedure, and there must be continuity between the conductance expressions for $T \gg T_d$ and $T_l \ll T \ll T_d$ at $T = T_d$. Thus, we get the conductance expression in this regime as

$$g = \frac{e^2}{h}[1 - \tilde{c}_2 V_1^2(\frac{T_d}{\Lambda})^{2(K_{eff}-1)})(\frac{T}{T_d})^{2(\tilde{K}_{eff}-1)}] \quad \text{for} \quad T_l \ll T \ll T_d \ , \tag{77}$$

where $\tilde{c}_2$ is a constant similar in nature to $\tilde{c}_1$, but it can depend on v_W and is hence dependent on the gate voltage V_G. Thus the conductance is no longer independent of V_G. This again is the same as the expression obtained by the explicit computation of the conductance.

Finally, in the low temperature limit, we recognize the fact that there is phase coherence over the distance between the two barriers; this follows from the low frequency effective action which has cross terms between the fields at the two barriers. This is what leads to resonant transmission. To compute the conductance corrections away from resonance in this limit, we note the following. Since the resonance occurs precisely when the $2k_F$ component of the barrier term goes to zero, the relevant term away from this resonance is precisely the back-scattering potential $V\cos(2\sqrt{\pi}\chi)$. Computing the dimension of this operator gives us the RG equation for our barriers in this temperature regime as

$$\frac{dV_1}{d\lambda} = (1 - K_L)V_1. \tag{78}$$

This makes the T dependence of the conductance correction clear. Again, the appearance of the energy scale v_W/l (through U_W) and the approximation $\bar{\omega}_n \ll U_W$ indicate that v_W/l has now replaced v_C/d as the high energy cutoff in the expression for the T dependence of the conductance correction. As before, the influence of those degrees of freedom whose energies lie in between v_W/l and v_C/d is shown by the appearance of the term $(T_l/T_d)^{2(\tilde{K}_{eff}-1)}$. This is because these degrees of freedom have also been integrated away during the RG procedure, and there must be continuity in the conductance expressions at $T = T_l$ whether we come from the $T_d \gg T \gg T_l$ regime or the $T_l \ll T$ regime. Thus, we obtain the conductance in this regime as

$$G = \frac{e^2}{h}[1 - \tilde{c}_3 V_1^2 (\frac{T_d}{\Lambda})^{2(K_{eff}-1)})(\frac{T_l}{T_d})^{2(\tilde{K}_{eff}-1)}(\frac{T}{T_l})^{2(K_L-1)}] \quad \text{for} \quad T \gg T_L \ , \tag{79}$$

where $\tilde{c}_3$ is a constant similar in nature to $\tilde{c}_2$. We can now see that, as $K_L = 1$ (for 2DEG Fermi reservoirs), the conductance has no temperature dependence in the low temperature regime.

A similar analysis can be done for the QPC limit, which reproduces the conductance expressions for the QPC limit that were obtained explicitly in the earlier subsection. We note, however, that the conductance corrections are small in this case as the RG flow for the barriers is restricted by the small length scales in the system.

The conductance corrections for electrons with spin can also be obtained using the effective actions and the RG equations for the barriers, by proceeding in the same way as was done for spinless electrons. Since the conductance expressions have already been given in the previous section, we do not repeat them here.

Thus, we emphasize that just by using the effective action and the RG equations for the barriers, we can actually obtain the conductance corrections. However, all that we actually do here is to compute the RG flows of the individual barriers, and then infer the temperature and length power-laws in the conductance corrections. Hence, even in

principle, there is no way of obtaining the constants $\tilde{c}_1, \ldots, \tilde{c}_6$ from this method, whereas the explicit computation of the conductance in the earlier subsection can give the explicit forms of the constants as well. In fact, the correlation functions computed there can be directly related to the coefficients which appear in the RG equations. In the various frequency regimes, the RG equation for a single barrier for spinless fermions can be written as

$$\frac{dV}{d\lambda} = (1 - 2|\bar{\omega}|G_{\bar{\omega}}(x,x))V. \tag{80}$$

On Fourier transforming, this gives

$$\frac{dV(x)}{d\lambda} = (1 + 2\frac{dG}{d\lambda}(x,x,\tau_0 e^{\lambda}))V(x) \ , \tag{81}$$

where τ_0 is the high energy cutoff $1/\Lambda$. Integrating this gives the renormalized strength of the impurity V_{ren} as

$$V_{ren}(x,\lambda) = V(x,\lambda=0)\exp[\lambda - U(x,x,\tau_0 e^{\lambda})] \ , \tag{82}$$

where $U(x,x,\tau_0 e^{\lambda}) = -2(G_0(x,x,\tau_0 e^{\lambda}) - G_0(x,x,\tau_0))$. Thus, in this case,

$$\chi_1(x,x) = \exp[l - U(x,x,\tau_0 e^{\lambda})] \ . \tag{83}$$

However, the non-local $\chi_1(x,y)$ is not so easy to obtain just from the RG equations.

Now, let us study the conclusions that can be drawn from the conductance expressions. To begin with, the expressions in the various frequency regimes reveal that as *either* the temperature T is raised *or* the total length L of the contacts and QW is decreased, the conductance corrections become smaller and the conductance approaches integer multiples of $2g_0$ as expected [3, 4]. Furthermore, we can see from these expressions that in the high temperature limit i.e., when $T \gg T_d,\ T_l$, the conductance corrections are independent of the QW parameters. Hence, they are *independent* of the gate voltage V_G and of all factors dependent on the channel index. Thus they yield renormalizations to the ideal values which are themselves plateau-like and uniform for all channels. Such corrections to the conductance explain some of the puzzling features observed in the experiments of Ref. [4]. A more detailed comparison of these results against experimental findings will be made in a later section; it is important to note here that our results are in qualitative agreement with most experimental observations on electronic transport through a variety of quantum wire systems.

Let us now compare these observations with what we find as the perturbative renormalizations to the perfect conductance of a barrier/impurity placed anywhere within the quantum wire itself such that its distance from the left lead-contact junction (taken as the origin) is again denoted by a. An exactly similar computation of the one-point Green's

function in this case reveals that (note that we are now working with the hierarchy of $d \ll a \ll l$)

$$G_{\bar{\omega}}(x = a, y = a) \simeq \frac{K}{2|\bar{\omega}|} \ , \tag{84}$$

where

$$K = \begin{cases} K_W & \text{for } |\bar{\omega}| \gg v_C/d \\ K_W & \text{for } v_W/a \ll |\bar{\omega}| \ll v_C/d \\ \frac{2K_L K_W}{K_L + K_W} & \text{for } v_W/l \ll |\bar{\omega}| \ll v_C/a \\ K_L & \text{for } |\bar{\omega}| \ll v_W/l \ . \end{cases}$$

Now, for a barrier at the left contact-QW junction, $a \to d$, the second frequency regime of $v_W/a \ll |\bar{\omega}| \ll v_C/d$ does not exist. We also find that $K = K'_{eff} \equiv 2K_C K_W/(K_C + K_W)$ rather than K_W for $|\bar{\omega}| \gg v_C/d$. Thus for a quantum wire system which has the two contact regions and only barriers at the two contact-QW junctions, the conductance in the highest temperature regime of $T \gg T_d$ is

$$g = g_0 K_L[1 - \tilde{c}_1(\frac{T}{\Lambda})^{2(K'_{eff}-1)}(|V(d)|^2 + |V(l+d)|^2)] \ . \tag{85}$$

Here $\tilde{c}_1$ is a dimensionful constant which will depend on factors like v_W and hence also the gate voltage V_G. For the intermediate temperature regime of $T_l \ll T \ll T_d$, we find the conductance to be

$$g = g_0 K_L[1 - \tilde{c}_2(\frac{T_d}{\Lambda})^{2(K'_{eff}-1)}(\frac{T}{T_d})^{2(\tilde{K}_{eff}-1)}(|V(d)|^2 + |V(l+d)|^2)] \ , \tag{86}$$

where $\tilde{K}_{eff} = 2K_L K_W/(K_L + K_W)$ as before, and $\tilde{c}_2$ is also a dimensionful constant dependent on V_G. Finally, for the lowest temperature regime of $T \ll T_l$, we obtain

$$g = g_0 K_L[1 - \tilde{c}_3(\frac{T}{T_l})^{2(K_L-1)}(\frac{T_d}{\Lambda})^{2(K'_{eff}-1)}(\frac{T_l}{T_d})^{2(\tilde{K}_{eff}-1)}|V(0) + V(l+2d)|^2] \ , \tag{87}$$

where $\tilde{c}_3$ too is a dimensionful constant dependent on V_G. Thus, we can see that any barrier or impurity placed anywhere inside the QW will always give a perturbative renormalization to the conductance which will be dependent on the gate voltage and hence can *never* be flat or even channel independent. The conductance expressions for the case of spinful electrons can be found for this case in exactly the same way as before.

5 Effects of a Magnetic Field

In this section, we will study the effects of an in-plane magnetic field on the conductivity of a quantum wire. In general, a magnetic field couples to both the spin (Zeeman coupling) and the orbital motion of an electron. However, orbital motion is not possible in an in-plane magnetic field because the electrons are constrained to move only in the plane. Thus we will only consider the effect of the Zeeman term. This term couples differently to spin up and spin down electrons; here up and down are defined with respect to the direction of the magnetic field which may or not be parallel to the quantum wire. Thus the $SU(2)$ symmetry of rotations is explicitly broken. We will now see that the spin and charge degrees of freedom do not decouple any longer. Our findings reveal that

(a) for low magnetic fields (of about $0 - 3T$ for Ga-As systems), the Zeeman splitting of the Fermi energies of the two spin species of electrons in the QW is very small, and its effects can be ignored.

(b) for intermediate magnetic fields (of about $3 - 8T$), the Zeeman splitting of the Fermi energies of up and down spins becomes appreciable; up and down spins see the two barrier strengths renormalize differently because of the Zeeman splitting, giving rise to an odd-even effect in the conductance of the two spin species.

(c) at still higher magnetic fields (of about $8 - 16T$), when each of the earlier sub-bands is completely Zeeman split into two spin-split sub-bands, conductance steps will be seen in multiples of $g_0 = e^2/h$; the odd-even effect will be most pronounced here with odd numbered spin-split sub-bands (containing only aligned moments) having a much less renormalized conductance and even numbered spin-split sub-bands (containing only anti-aligned moments) having a much more renormalized conductance, and we can treat each spin-split sub-band as an effectively spinless TLL system.

(d) at magnetic fields much higher than this, all the spins in the system will be spin polarized.

5.1 The infinite TLL Quantum Wire and the Odd-Even Effect

Let us first consider an infinitely long wire containing noninteracting electrons. A magnetic field h contributes the following term to the Hamiltonian

$$- \; g\mu_B h \; S_{z,total} \;=\; - \; \frac{g\mu_B h}{2} \; (\; \rho_{0\uparrow} \; + \; \frac{1}{\sqrt{\pi}} \; \partial_x \phi_\uparrow \; - \; \rho_{0\downarrow} \; - \; \frac{1}{\sqrt{\pi}} \; \partial_x \phi_\downarrow \;) \; , \qquad (88)$$

where g is the gyromagnetic ratio (which is 2 for free electrons but may be substantially smaller in quantum wire systems), $\rho_{0\uparrow}, \rho_{0\downarrow}$ respectively denote the mean density of the

spin up and spin down electrons, and $\phi_\uparrow, \phi_\downarrow$ denote the bosonic fields for the spin up and down electrons. The density terms $\rho_{0\sigma} = \rho_{0\uparrow} - \rho_{0\downarrow}$ have a bigger effect than the derivative terms $\partial_x \phi_\sigma$; by altering the chemical potentials for spin up and down electrons, these terms lead to different Fermi momenta and therefore to different Fermi velocities $v_{F\uparrow}$ and $v_{F\uparrow}$ for the two kinds of electrons.

We now add a density-density interaction of the form $\mathcal{U}\rho^2/2$ where $\rho = \rho_\uparrow + \rho_\downarrow$. (For instance, this may describe a short-range Coulomb repulsion as in the Hubbard model; in that case $\mathcal{U}$ is positive). The bosonized Lagrangian density takes the form

$$\begin{aligned} \mathcal{L} \;=\; & \frac{1}{2v_{F\uparrow}} \, (\partial_t \phi_\uparrow)^2 \;-\; \frac{v_{F\uparrow}}{2} \, (\partial_x \phi_\uparrow)^2 \;+\; \frac{1}{2v_{F\downarrow}} \, (\partial_t \phi_\downarrow)^2 \;-\; \frac{v_{F\downarrow}}{2} \, (\partial_t \phi_\downarrow)^2 \\ & - \frac{\mathcal{U}}{2\pi} \, (\, \partial_x \phi_\uparrow \;+\; \partial_x \phi_\downarrow \,)^2 \, , \end{aligned} \tag{89}$$

where we have dropped some additive constants, and have only kept terms which are quadratic in the fields. We can rediagonalize this Lagrangian by defining two new fields ϕ_i, velocities v_i and interaction parameters K_i (where $i = +, -$), and a mixing angle γ, where

$$\begin{aligned} \phi_+ \;&=\; \sqrt{K_+ v_+} \, (\frac{1}{\sqrt{v_{F\uparrow}}} \cos\gamma \; \phi_\uparrow + \frac{1}{\sqrt{v_{F\downarrow}}} \sin\gamma \; \phi_\downarrow) \equiv p\phi_\uparrow + q\phi_\downarrow, \\ \phi_- \;&=\; \sqrt{K_- v_-} \, (-\frac{1}{\sqrt{v_{F\uparrow}}} \sin\gamma \; \phi_\uparrow + \frac{1}{\sqrt{v_{F\downarrow}}} \cos\gamma \; \phi_\downarrow) \equiv r\phi_\uparrow + s\phi_\downarrow, \end{aligned} \tag{90}$$

and

$$\begin{aligned} v_+^2 \;+\; v_-^2 \;&=\; v_{F\uparrow}^2 \;+\; v_{F\downarrow}^2 \;+\; \frac{\mathcal{U}}{\pi} \, (\, v_{F\uparrow} \;+\; v_{F\downarrow} \,) \, , \\ (\, v_+^2 \;-\; v_-^2 \,) \, \cos \, (2\gamma) \;&=\; v_{F\uparrow}^2 \;-\; v_{F\downarrow}^2 \;+\; \frac{\mathcal{U}}{\pi} \, (\, v_{F\uparrow} \;-\; v_{F\downarrow} \,) \, , \\ (\, v_+^2 \;-\; v_-^2 \,) \, \sin \, (2\gamma) \;&=\; \frac{2\mathcal{U}}{\pi} \, \sqrt{v_{F\uparrow} v_{F\downarrow}} \, , \\ K_+ v_+ \, (\, \frac{\cos^2\gamma}{v_{F\uparrow}} \;+\; \frac{\sin^2\gamma}{v_{F\downarrow}} \,) \;&=\; 1 \, , \\ K_- v_- \, (\, \frac{\sin^2\gamma}{v_{F\uparrow}} \;+\; \frac{\cos^2\gamma}{v_{F\downarrow}} \,) \;&=\; 1 \, . \end{aligned} \tag{91}$$

The Lagrangian density in Eq. (89) then takes the decoupled form

$$\mathcal{L} \;=\; \frac{1}{2K_+ v_+} \, (\partial_t \phi_+)^2 \;-\; \frac{v_+}{2K_+} \, (\partial_x \phi_+)^2 \;+\; \frac{1}{2K_- v_-} \, (\partial_t \phi_-)^2 \;-\; \frac{v_-}{2K_-} \, (\partial_t \phi_-)^2 \, . \tag{92}$$

Thus the charge and spin degrees of freedom get mixed since the fields ϕ_+ and ϕ_- which diagonalize the Lagrangian will generally be different from the fields $\phi_\rho = (\phi_\uparrow + \phi_\downarrow)/\sqrt{2}$ and $\phi_\sigma = (\phi_\uparrow - \phi_\downarrow)/\sqrt{2}$. Note that if the magnetic field h is zero, then $v_{F\uparrow} = v_{F\downarrow}$ and $\gamma = \pi/4$; ϕ_+ and ϕ_- are then identical (up to a sign) to the charge and spin fields ϕ_ρ and ϕ_σ.

We will now present the RG equations for a weak δ-function impurity placed at the origin. For this, we need to compute the scaling dimension of the impurity term in the Lagrangian. We first write the impurity term in terms of fermionic fields $\psi_\uparrow(0)$ and $\psi_\downarrow(0)$, and then in terms of the bosonic fields $\phi_\uparrow(0)$ and $\phi_\downarrow(0)$ at the origin as

$$\begin{aligned} L_{imp} &= V(0)(\psi_\uparrow^\dagger(0)\psi_\downarrow(0) + \psi_\downarrow^\dagger(0)\psi_\uparrow(0)) \\ &= V_1\Lambda\,[\cos(2\sqrt{\pi}\phi_\uparrow(0)) + \cos(2\sqrt{\pi}\phi_\downarrow(0))]\ . \end{aligned} \tag{93}$$

We then invert the relations between $\phi_\pm$ and $\phi_{\uparrow,\downarrow}$ given above in order to rewrite the above expression for the impurity in terms of the diagonal fields $\phi_\pm$. The scaling dimensions of the impurity terms are then found to be

$$D_{V_\uparrow} = v_{F\uparrow}(\frac{\cos^2\gamma}{v_+} + \frac{\sin^2\gamma}{v_-}) \quad , \quad D_{V_\downarrow} = v_{F\downarrow}(\frac{\sin^2\gamma}{v_+} + \frac{\cos^2\gamma}{v_-}). \tag{94}$$

Hence the RG equations for $V_\uparrow$ and $V_\downarrow$ are given by

$$\begin{aligned} \frac{dV_\uparrow}{d\lambda} &= (1 - D_{V_\uparrow})V_\uparrow \\ \frac{dV_\downarrow}{d\lambda} &= (1 - D_{V_\downarrow})V_\downarrow\ , \end{aligned} \tag{95}$$

where $V_\uparrow$ and $V_\downarrow$ both start from the value V_1 at the microscopic length scale.

We can now study what happens in the presence of strong and weak magnetic fields. But let us first remind ourselves of the following relations (which result from the Zeeman splitting),

$$\begin{aligned} v_{F\uparrow,\downarrow} &= v_F\sqrt{1 \pm \frac{g\mu_B h}{2E_{F1D}}} \\ \tan(2\gamma) &= \frac{2\mathcal{U}\sqrt{v_{F\uparrow}v_{F\downarrow}}/\pi}{(v_{F\uparrow} - v_{F\downarrow})(v_{F\uparrow} + v_{F\downarrow} + \mathcal{U}/\pi)}\ , \end{aligned} \tag{96}$$

where $v_F = \sqrt{2E_{F1D}/m}$ is the Fermi velocity in the absence of a magnetic field. Therefore, in the limit of a strong magnetic field where the Zeeman splitting of the two spin species is much larger than the short ranged interaction energy $\mathcal{U}$ (i.e., $\mathcal{U} \ll |v_{F\uparrow} - v_{F\downarrow}|$ and

$\gamma \ll \pi/2$), we can approximate the relations for the two velocities $v_\pm$ (to linear order in $\mathcal{U}/(v_{F\uparrow} - v_{F\downarrow})$) as

$$\begin{aligned} v_+ &= v_{F\uparrow} + \delta_+ \quad , \quad \delta_+ \ll v_{F\uparrow} \\ v_- &= v_{F\downarrow} + \delta_- \quad , \quad \delta_- \ll v_{F\downarrow} \ . \end{aligned} \tag{97}$$

By putting these relations for $v_\pm$ into the expressions given above relating $v_\pm$ and $v_{F\uparrow,\downarrow}$, we get

$$\delta_+ \ = \ \delta_- \ = \ \frac{\mathcal{U}}{2\pi} \ . \tag{98}$$

Now, using this (together with the fact that $\gamma \ll \frac{\pi}{2}$) in the two RG equations obtained above gives us

$$\begin{aligned} \frac{dV_\uparrow}{d\lambda} &= (1 - \frac{v_{F\uparrow}}{v_+})V_\uparrow \\ &\simeq \frac{\mathcal{U}}{2\pi v_{F\uparrow}} V_\uparrow \ , \end{aligned} \tag{99}$$

and

$$\begin{aligned} \frac{dV_\downarrow}{d\lambda} &= (1 - \frac{v_{F\downarrow}}{v_-})V_\downarrow \\ &\simeq \frac{\mathcal{U}}{2\pi v_{F\downarrow}} V_\downarrow \ . \end{aligned} \tag{100}$$

Now, these two RG equations indicate that as $v_{F\uparrow}$ is larger than $v_{F\downarrow}$, the renormalized impurity strength felt by those electrons which have their magnetic moments aligned with the external B field is less than the renormalized impurity strength felt by the electrons which have their magnetic moments anti-aligned with the B field. Furthermore, if the B field is further increased, we will reach a situation when alternate sub-bands in the QW will be populated by either only the aligned or only the anti-aligned electrons. In this regime, the difference in back-scattering felt by the two species of electrons will be very clear from the alternating weak and strong corrections to the conductance. To be more specific, all odd numbered sub-bands will show much less corrections to the perfect conductance (as they will be populated by electrons aligned with the magnetic field), while all even numbered sub-bands will show much greater corrections to the perfect conductance (as they will be populated by the anti-aligned electrons). This *odd-even* effect had, in fact, been predicted by a two-band TLL study of Kimura *et al* [28], but its explanation on the grounds of impurity renormalization is now made clear. Furthermore, this effect has been recently observed by Liang *et al* [7], and we will discuss their observations in a later section. It should be noted here that though the odd-even effect is easy to show upon

taking the limit of $\mathcal{U} \ll |v_{F\uparrow} - v_{F\downarrow}|$, the existence of this phenomenon does not need this limit to be taken. Furthermore, we also find that upon taking the limit of $h \ll E_{F1D}$ (i.e., weak magnetic field with $v_{F\uparrow} = v_{F\downarrow} = v_F$),

$$\frac{dV_\uparrow}{d\lambda} = \frac{dV_\downarrow}{d\lambda} = \frac{\mathcal{U}}{2\pi v_F} \ , \tag{101}$$

which tells us that the odd-even effect vanishes in the weak magnetic field limit. Finally, we comment on the fact that the odd-even effect discussed above gives rise to the possibility of the creation of a spin-valve (i.e., a spin polarized current creating device) in these QW systems. Even though the odd-even effect needs a high magnetic field to be observed in current day experiments [7], it may be possible to employ artificial barriers like negatively-biased finger gates to heighten the difference in renormalization of the up and down spin electrons at lower magnetic fields. At this point, however, quantitative predictions are difficult to make.

5.2 A study of our model for the QW with a magnetic field

Having discussed how to obtain a diagonal Lagrangian when both a magnetic field and interactions are present as well as shown the interesting odd-even effect that takes place because of an impurity in an infinite TLL in the presence of an external B field, we will now study what happens when the model in Sec. 2 is placed in a magnetic field. In the regions $x < 0$ and $x > l + 2d$, we have a system of noninteracting electrons parametrized by velocities $v_{F\uparrow}$ and $v_{F\downarrow}$. In the regions of the contacts $0 < x < d$ and $l + d < x < l + 2d$, we have an interacting system parametrized by two velocities v_{C+}, v_{C-} and a mixing angle γ_C. In the quantum wire $d < x < l + d$, the system is parametrized by the velocities v_{W+}, v_{W-} and a mixing angle γ_W. The last six parameters are functions of $v_{F\uparrow}$, $v_{F\downarrow}$ and the strengths of the interaction in the contacts and quantum wire. The action for this model is given by

$$\begin{aligned} S_0 &= \int d\tau \, [\int_{-\infty}^{0} + \int_{l+2d}^{\infty}] \, dx \, \{ \, \frac{1}{2K_L}[\frac{1}{v_{F\uparrow}}(\partial_\tau \phi_\uparrow)^2 + v_{F\uparrow}(\partial_x \phi_\uparrow)^2] \; + \; [\uparrow \rightarrow \downarrow] \, \} \\ &+ \int d\tau \, [\int_{0}^{d} + \int_{l+d}^{l+2d}] \, dx \, \{ \, \frac{1}{2K_{C+}}[\frac{1}{v_{C+}}(\partial_\tau \phi_{C+})^2 + v_{C+}(\partial_x \phi_{C+})^2] \; + \; [C+ \rightarrow C-] \, \} \\ &+ \int d\tau \, \int_{d}^{l+d} dx \, \{ \, \frac{1}{2K_{W+}}[\frac{1}{v_{W+}}(\partial_\tau \phi_{W+})^2 + v_{W+}(\partial_x \phi_{W+})^2] \; + \; [W+ \rightarrow W-] \, \} \ . \end{aligned} \tag{102}$$

Note that we have ignored the junction barriers and the gate voltage for the moment. It is worth mentioning here that we have verified, by performing a calculation of the

kind outlined in Ref. [17], that our model for the QW system when placed in an external magnetic field and in the absence of any barriers/impurities still gives perfect conductance in the dc limit for each sub-band.

We begin by noting that we will present here the calculation for the case when the mixing angle γ is the same in both the contacts as well as the QW, i.e., the short ranged electron-electron interaction $\mathcal{U}$ is equal in all the three TLLs. Though this is not necessarily the case in a real system, we will present it as it considerably simplifies the computations while providing us with an adequate discussion of all the important results for effective actions, conductance expressions, resonances, etc. Later, we will briefly discuss the case in which the mixing angle is different in the contact and QW regions. The explicit derivation of the effective action is given in Appendix C. The high frequency effective Lagrangian density ($\bar{\omega} \gg v_{C\pm}/d, v_{W\pm}/l$) simplifies to

$$\begin{aligned}
\mathcal{L}_{eff,high} &= \frac{|\bar{\omega}|}{2}[(\frac{1}{K_L}+\frac{p^2}{K_{C+}}+\frac{r^2}{K_{C-}})(\tilde{\phi}_{1\uparrow}^2+\tilde{\phi}_{4\uparrow}^2)+(\frac{1}{K_L}+\frac{q^2}{K_{C+}}+\frac{s^2}{K_{C-}})(\tilde{\phi}_{1\downarrow}^2+\tilde{\phi}_{4\downarrow}^2) \\
&\quad + 2(\frac{pq}{K_{C+}}+\frac{rs}{K_{C-}})(\tilde{\phi}_{1\uparrow}\tilde{\phi}_{1\downarrow}+\tilde{\phi}_{4\uparrow}\tilde{\phi}_{4\downarrow})] \\
&+ \frac{|\bar{\omega}|}{2}[\{p^2(\frac{1}{K_{C+}}+\frac{1}{K_{W+}})+r^2(\frac{1}{K_{C-}}+\frac{1}{K_{W-}})\}(\tilde{\phi}_{2\uparrow}^2+\tilde{\phi}_{3\uparrow}^2) \\
&\quad + \{q^2(\frac{1}{K_{C+}}+\frac{1}{K_{W+}})+s^2(\frac{1}{K_{C-}}+\frac{1}{K_{W-}})\}(\tilde{\phi}_{2\downarrow}^2+\tilde{\phi}_{3\downarrow}^2) \\
&\quad + 2\{pq(\frac{1}{K_{C+}}+\frac{1}{K_{W+}})+rs(\frac{1}{K_{C-}}+\frac{1}{K_{W-}})\}(\tilde{\phi}_{2\uparrow}\tilde{\phi}_{2\downarrow}+\tilde{\phi}_{3\uparrow}\tilde{\phi}_{3\downarrow})] \\
&+ \mathcal{L}_{gate}(\phi_{2\uparrow,\downarrow},\phi_{3\uparrow,\downarrow})+\mathcal{L}_{imp}(\phi_{1\uparrow,\downarrow},\phi_{4\uparrow,\downarrow}). \qquad (103)
\end{aligned}$$

We can clearly see the separation between the outer two and inner two fields. This means that we can integrate out the inner fields $\tilde{\phi}_{2\uparrow,\downarrow}$ and $\tilde{\phi}_{3\uparrow,\downarrow}$ without any further work and be left with a high frequency effective action dependent on $\tilde{\phi}_{1\uparrow,\downarrow}$ and $\tilde{\phi}_{4\uparrow,\downarrow}$ exactly as given above (and without any influence of the gate voltage V_G either). We can also make the prediction that the conductance corrections due to barriers at the outer two junctions will have temperature power-laws which will be combinations of K_L and $K_{C\pm}$ (much like those seen before) and also that it will be not be dependent on the gate voltage.

In the intermediate frequency range of $v_{W\pm}/l \ll \bar{\omega} \ll v_{C\pm}/d$, we get (after integrating out the inner fields $\tilde{\phi}_{2\uparrow,\downarrow}$ and $\tilde{\phi}_{3\uparrow,\downarrow}$),

$$\begin{aligned}
\mathcal{L}_{eff,int} &= \frac{|\bar{\omega}|}{2}[(\frac{1}{K_L}+\frac{p^2}{K_{W+}}+\frac{r^2}{K_{W-}})(\tilde{\phi}_{1\uparrow}^2+\tilde{\phi}_{4\uparrow}^2)+(\frac{1}{K_L}+\frac{q^2}{K_{W+}}+\frac{s^2}{K_{W-}})(\tilde{\phi}_{1\downarrow}^2+\tilde{\phi}_{4\downarrow}^2) \\
&\quad + 2(\frac{pq}{K_{W+}}+\frac{rs}{K_{W-}})(\tilde{\phi}_{1\uparrow}\tilde{\phi}_{1\downarrow}+\tilde{\phi}_{4\uparrow}\tilde{\phi}_{4\downarrow})]
\end{aligned}$$

$$+\frac{\tilde{V}_G(p-q)(s-r)}{(ps-qr)}(\phi_{4\uparrow}-\phi_{1\uparrow}+\phi_{4\downarrow}-\phi_{1\downarrow})\ , \tag{104}$$

where $\alpha_{C\pm}=v_{C\pm}/(K_{C\pm}d)$ are the charging energies for the $\tilde{\phi}_\pm$ fields, and they appear because of the growth of the coherence in the system over the contact regions. We can now predict that the conductance corrections due to barriers at the outer two junctions will have temperature power-laws which will be combinations of K_L and $K_{W\pm}$ (again like those seen previously), and that this correction will definitely be dependent on the gate voltage.

Finally, in the low frequency limit of $\bar{\omega}\ll v_{W\pm}/l$, we get

$$\begin{aligned}\mathcal{L}_{eff,low} &= \frac{|\bar{\omega}|}{2K_L}(\tilde{\phi}^2_{1\uparrow}+\tilde{\phi}^2_{1\downarrow}+\tilde{\phi}^2_{4\uparrow}+\tilde{\phi}^2_{4\downarrow})\\ &+\sum_\pm \frac{v_{C\pm}}{2d}[\phi^2_{2\pm}+\phi^2_{3\pm}+\phi^2_{1\pm}+\phi^2_{4\pm}-2\phi_{2\pm}\phi_{1\pm}-2\phi_{3\pm}\phi_{4\pm}]\\ &+\sum_\pm \frac{v^2_{W\pm}}{2lv_{C\pm}}(\phi_{2\pm}-\phi_{3\pm})^2\\ &+\sum_\pm \frac{\tilde{V}_G}{2(ps-qr)}[(s-r)(\phi_{3+}-\phi_{2+})+(p-q)((\phi_{3-}-\phi_{2-})].\end{aligned} \tag{105}$$

Integrating out the inner fields, we are then left with an effective action in terms of the new current and charge variables respectively

$$\begin{aligned}\phi_{14\uparrow,\downarrow} &= \frac{\phi_{1\uparrow,\downarrow}+\phi_{4\uparrow,\downarrow}}{2}\\ n_{14\uparrow,\downarrow} &= \frac{\phi_{4\uparrow,\downarrow}-\phi_{1\uparrow,\downarrow}}{\sqrt{\pi}}\ .\end{aligned} \tag{106}$$

that span the coherent TLL system between the two lead-contact junction barriers in this low frequency regime. Thus, we get the effective Lagrangian density in this regime as

$$\begin{aligned}\mathcal{L}_{eff,low} &= \frac{|\bar{\omega}|}{K_L}[\tilde{\phi}^2_{14\uparrow}+\tilde{\phi}^2_{14\downarrow}+\frac{\pi}{4}\tilde{n}^2_{14\uparrow}+\frac{\pi}{4}\tilde{n}^2_{14\downarrow}]\\ &+\frac{U_1}{2}(pn_{14\uparrow}+qn_{14\downarrow}+n_{01})^2+\frac{U_2}{2}(rn_{14\uparrow}+sn_{14\downarrow}+n_{02})^2+\mathcal{L}_{imp},\end{aligned} \tag{107}$$

where

$$U_1 = \frac{\pi v_{W+}\alpha_+\beta_+}{v_{C+}\alpha_++2v_{W+}\beta_+}\ ,\ U_2=\frac{\pi v_{W-}\alpha_-\beta_-}{v_{C-}\alpha_-+2v_{W-}\beta_-}$$

$$
\begin{aligned}
n_{01} &= \frac{\tilde{V}_G v_{C+}(s-r)}{\pi v_{W+}\beta_+(ps-qr)} \quad , \quad n_{02} = \frac{\tilde{V}_G v_{C-}(p-q)}{\pi v_{W-}\beta_-(ps-qr)} \\
\text{and} \quad \alpha_\pm &= \frac{v_{C\pm}}{K_{C\pm}d} \quad , \quad \beta_\pm = \frac{v_{W\pm}}{K_{W\pm}d},
\end{aligned} \tag{108}
$$

and the term coming from the two barriers can be written as

$$
\mathcal{L}_{imp} = 2V\Big(\cos(2\sqrt{\pi}\phi_{14\uparrow})\cos(\pi n_{14\uparrow}) + \cos(2\sqrt{\pi}\phi_{14\downarrow})\cos(\pi n_{14\downarrow})\Big) \ . \tag{109}
$$

It becomes clear from the above expression that the temperature power-law will be dependent on the lead interaction parameter $K_L = 1$, and the conductance correction will, in this regime, be temperature independent (as seen previously). Furthermore, the length corrections will be gate voltage dependent. Let us now study the possible resonance symmetries of the low frequency effective action given above. Even though the structure of this expression is more complicated than those encountered previously, we can rewrite the two charging terms as follows:

$$
\mathcal{L}_{charging} = \frac{(U_1 p^2 + U_2 r^2)}{2}[n_{14\uparrow} + a n_{14\downarrow} - b]^2 + f(n_{14\downarrow}) + \text{const} \ , \tag{110}
$$

where

$$
\begin{aligned}
a &= \frac{U_1 pq + U_2 rs}{U_1 p^2 + U_2 r^2} \\
b &= \frac{U_1 n_{01} + U_2 n_{02}}{U_1 p^2 + U_2 r^2} \ ,
\end{aligned} \tag{111}
$$

and $f(n_{14\downarrow})$ is a quadratic function of the field $n_{14\downarrow}$ only. Thus, we can see that if we set

$$
a n_{14\downarrow} - b = -Z - \frac{1}{2} \ , \tag{112}
$$

we get a resonance in the $n_{14\uparrow}$ parts of the charging and barrier terms whenever $n_{14\uparrow} = Z$ or $Z+1$ and one makes the transformation of $\phi_{14\uparrow} \to \phi_{14\uparrow} \pm \sqrt{\pi}/2$. This means that only the transport of all up-spin electrons through the two barriers is at resonance, and this is clearly a one-parameter tuned resonance. A one-parameter tuned resonance for only the transport of all down-spin electrons through the two barriers can be found in exactly the same manner by rewriting the above charging expressions but for $n_{14\downarrow}$ instead of $n_{14\uparrow}$. We also find another resonance given by

$$
\begin{aligned}
\frac{q}{p} n_{14\downarrow} + \frac{1}{p} n_{01} &= -Z - \frac{1}{2} \ , \\
\text{and} \quad \frac{s}{r} n_{14\downarrow} + \frac{1}{r} n_{02} &= -Z - \frac{1}{2} \ ,
\end{aligned} \tag{113}
$$

where Z is the same integer in both equations; then there exists a possible resonance whenever $n_{14\uparrow} = Z$ or $Z+1$, and one makes the transformation of $\phi_{14\uparrow,\downarrow} \to \phi_{14\uparrow,\downarrow} \pm \sqrt{\pi}/2$. This resonance symmetry would lead to a vanishing of the barrier terms in the effective action, and would correspond to the transfer of an electron across the system. One can immediately see that the above two conditions on $n_{14\downarrow}$ mean that two parameters, here the gate voltage V_G and the external magnetic field h, have to be manipulated to achieve this resonance condition. Such a resonance will, therefore, be much more difficult to observe experimentally. However, this resonance will lead to a complete vanishing of all back-scattering (and hence the conductance corrections) while the two one-parameter tuned resonances will give only partial lessening of the conductance corrections.

The two one-parameter tuned resonances can prove useful in creating a spin-valve. Even at a low magnetic field, the odd-even effect can be enhanced by using stronger artificial barriers (e.g., by employing finger gates over the channel) or making the length of the channel longer or working at lower temperatures, together with tuning the transport of only one spin species of electrons through the two barriers at resonance. Thus one can create an enhanced spin polarized electron current output from the QW system.

Before we go on to computing the conductance through the system for the above model in the presence of the magnetic field, let us make some remarks about the case when the mixing angle in the QW is taken to be different from that in the contacts. A long calculation does give expressions for the effective action in the three frequency regimes similar to those obtained above, but with two sets of the transformation coefficients relating the $\phi_{\pm}$ and $\phi_{\uparrow,\downarrow}$ fields. However, the integrating out of the inner fields is a far more difficult task; furthermore, the analysis reveals that the only possible resonance symmetry of the low frequency effective action is one that needs at least four parameters to be manipulated. We will, therefore, not present these results as we do not find anything substantially new from the analysis compared to the simpler case of equal mixing angles.

5.3 Conductance of our model for the QW with a magnetic field

We will begin by a re-writing the RG equation, obtained by Safi and Schulz [24] for an impurity placed within a QW of a finite size and connected to Fermi leads, in a way which will be convenient to use in computing the conductance expressions for our model of the QW with barriers even in the presence of the external magnetic field. We begin by quoting the expression for the RG flow found for an impurity in Ref. [24],

$$\frac{dV_{m_\rho,m_\sigma}(x)}{d\lambda} = [1 - \frac{1}{2}(m_\rho^2 \frac{dU_\rho(x,x,\tau_0 e^\lambda)}{d\lambda} + m_\sigma^2 \frac{dU_\sigma(x,x,\tau_0 e^\lambda)}{d\lambda})]V_{m_\rho,m_\sigma}(x), \qquad (114)$$

where

$$\begin{aligned} U_\rho(x,x,\tau_0 e^\lambda) &= 2[G_\rho(x,x,\tau_0) - G_\rho(x,x,\tau_0 e^\lambda)] \\ U_\sigma(x,x,\tau_0 e^\lambda) &= 2[G_\sigma(x,x,\tau_0) - G_\sigma(x,x,\tau_0 e^\lambda)]. \end{aligned} \tag{115}$$

Now with $\phi_\rho = (\phi_\uparrow + \phi_\downarrow)/\sqrt{2}$ and $\phi_\sigma = (\phi_\uparrow - \phi_\downarrow)/\sqrt{2}$, we can write

$$\begin{aligned} G_\rho(x,x,\tau_0 e^\lambda) &= <\phi_\rho(x,\tau_0 e^\lambda)\phi_\rho(x,0)> = \frac{1}{2}[<\phi_\uparrow\phi_\uparrow> + <\phi_\downarrow\phi_\downarrow> + 2<\phi_\uparrow\phi_\downarrow>] \\ G_\sigma(x,x,\tau_0 e^\lambda) &= <\phi_\sigma(x,\tau_0 e^\lambda)\phi_\sigma(x,0)> = \frac{1}{2}[<\phi_\uparrow\phi_\uparrow> + <\phi_\downarrow\phi_\downarrow> - 2<\phi_\uparrow\phi_\downarrow>], \end{aligned} \tag{116}$$

where the space-time indices are implicit on the right hand sides. Substituting the expressions for U_ρ and U_σ given above in the RG equation, and working with the case for the back-scattering of one electron $m_\rho = m_\sigma = 1$, we write the RG equation as

$$\frac{dV_{1,1}(x)}{d\lambda} = [1 + \frac{d}{d\lambda}(G_\uparrow(x,x,\tau_0 e^\lambda) + G_\downarrow(x,x,\tau_0 e^\lambda))]V_{1,1}(x) \ , \tag{117}$$

where $G_\uparrow = <\phi_\uparrow\phi_\uparrow>$ and $G_\downarrow = <\phi_\downarrow\phi_\downarrow>$. We will now use the effective actions found in the various frequency regimes to obtain the two Green's functions $G_\uparrow$ and $G_\downarrow$, put these in the RG equations and thereby infer the corrections to the conductance caused by the junction barriers.

We start with the high and intermediate frequency/temperature effective actions given earlier for the model when the mixing angle is the same in the contact and QW regions. Here, we can see that the final effective action (in terms of only the fields at the outer two junctions) is the sum of two distinct parts, each of which is an expression of the kind $\frac{A}{2}\phi_\uparrow^2 + \frac{B}{2}\phi_\downarrow^2 + C\phi_\uparrow\phi_\downarrow$ separately for fields ϕ_1 and ϕ_4. This tells us that we can simply take the sum of the contributions from each of the two incoherent barriers. Thus, the general expression

$$\mathcal{L}_{eff} = \frac{A}{2|\bar{\omega}|}\tilde{\phi}_\uparrow^2 + \frac{B}{2|\bar{\omega}|}\tilde{\phi}_\downarrow^2 + \frac{C}{|\bar{\omega}|}\tilde{\phi}_\uparrow\tilde{\phi}_\downarrow, \tag{118}$$

can be diagonalized in terms of two new fields ϕ_a and ϕ_b i.e., written as

$$\mathcal{L}_{eff} = \frac{1}{2|\bar{\omega}|}(\lambda_a\tilde{\phi}_a^2 + \lambda_b\tilde{\phi}_b^2) \ , \tag{119}$$

where λ_a and λ_b are the eigenvalues of the transformation given by

$$\lambda_{a,b} = \frac{A+B}{2} \pm \frac{1}{2}\sqrt{(A-B)^2 + C^2} \ . \tag{120}$$

Then,

$$\begin{aligned} G_{\bar{\omega}a} &= <\tilde{\phi}_a\tilde{\phi}_a> = \frac{1}{\lambda_a|\bar{\omega}|} \\ G_{\bar{\omega}b} &= <\tilde{\phi}_b\tilde{\phi}_b> = \frac{1}{\lambda_b|\bar{\omega}|}. \end{aligned} \tag{121}$$

Using the two eigenvectors corresponding to these two eigenvalues, we obtain $G_{\bar{\omega}\uparrow}$ and $G_{\bar{\omega}\downarrow}$ as

$$G_{\bar{\omega}\uparrow} = \frac{C^2}{|\bar{\omega}|\{(\lambda_a - A)(\lambda_b - B) - C^2\}^2}[C^2 G_{\bar{\omega}a} + (\lambda_b - B)^2 G_{\bar{\omega}b}], \tag{122}$$

and

$$G_{\bar{\omega}\downarrow} = \frac{C^2}{|\bar{\omega}|\{(\lambda_a - A)(\lambda_b - B) - C^2\}^2}[(\lambda_a - A)^2 G_{\bar{\omega}a} + C^2 G_{\bar{\omega}b}]. \tag{123}$$

We finally obtain an expression for $G_{\bar{\omega}\uparrow} + G_{\bar{\omega}\downarrow}$ as

$$\begin{aligned} G_{\bar{\omega}\uparrow} + G_{\bar{\omega}\downarrow} &= \frac{C^2}{|\bar{\omega}|\{(\lambda_a - A)(\lambda_b - B) - C^2\}^2}[\frac{C^2 + (\lambda_a - A)^2}{\lambda_a} + \frac{C^2 + (\lambda_b - B)^2}{\lambda_b}] \\ &\equiv \frac{K_{mag}}{2|\bar{\omega}|}. \end{aligned} \tag{124}$$

We can now use the Fourier transform of the above expression to obtain the temperature and length power-laws for the conductance corrections in the high and intermediate frequency regimes. In the high temperature regime of $T \gg T_d$ ($\sim v_{C\pm}/d$), we get the conductance as

$$g = g_0 K_L[1 - c_1(|V(0)|^2 + |V(l+2d)|^2)(\frac{T}{\Lambda})^{(K_{eff,mag}-2)}], \tag{125}$$

where c_1 is a dimensionful constant independent of the gate voltage V_G, and $K_{eff,mag}$ is given by the expression for K_{mag} where the coefficients A, B and C are given by

$$\begin{aligned} A &= \frac{1}{K_L} + \frac{p^2}{K_{C+}} + \frac{r^2}{K_{C-}} \\ B &= \frac{1}{K_L} + \frac{q^2}{K_{C+}} + \frac{s^2}{K_{C-}} \\ C &= \frac{pq}{K_{C+}} + \frac{rs}{K_{C-}}\ . \end{aligned} \tag{126}$$

Similarly, the conductance expression for the intermediate temperature defined by T_l ($\sim v_{W\pm}/l$) $\ll T \ll T_d$ is given by

$$g = g_0 K_L[1 - c_2(|V(0)|^2 + |V(l+2d)|^2)(\frac{\tilde{T}_d}{\Lambda})^{(K_{eff,mag}-2)}(\frac{T}{\tilde{T}_d})^{(\tilde{K}_{eff,mag}-2)}], \tag{127}$$

where c_2 is another dimensionful constant which is dependent on the gate voltage, T_d has replaced Λ as the correct cutoff for the temperature, and $\tilde{K}_{eff,mag}$ is found in exactly the same way as $K_{eff,mag}$ but with coefficients A_1, B_1 and C_1 defined as

$$\begin{aligned} A_1 &= \frac{1}{K_L} + \frac{p^2}{K_{W+}} + \frac{r^2}{K_{W-}} \\ B_1 &= \frac{1}{K_L} + \frac{q^2}{K_{W+}} + \frac{s^2}{K_{W-}} \\ C_1 &= \frac{pq}{K_{W+}} + \frac{rs}{K_{W-}}. \end{aligned} \tag{128}$$

Finally, we obtain the low frequency conductance expression for the temperature regime of $T \ll T_l$ as

$$g = g_0 K_L[1 - c_3(|V(0) + V(l+2d)|^2)(\frac{\tilde{T}_d}{\Lambda})^{(K_{eff,mag}-2)}(\frac{T_l}{T_d})^{(\tilde{K}_{eff,mag}-2)}(\frac{T}{T_l})^{2(K_L-1)}], \tag{129}$$

where c_3 is a dimensionful constant similar in nature to c_2, i.e., dependent on gate voltage. This expression is also independent of the temperature for Fermi leads with $K_L = 1$, and the coherence between the barriers means that this correction term could go to zero at resonance.

We end by noting that we can again take the limit of $\mathcal{U} \ll |v_{C\uparrow} - v_{C\downarrow}|$ in our equations to highlight the existence of the odd-even effect within our model of the QW as well. Upon taking this limit in the high temperature regime, we find that

$$\frac{dV_\uparrow}{d\lambda} \simeq \frac{\mathcal{U}}{4\pi v_{C\uparrow}}, \tag{130}$$

while

$$\frac{dV_\downarrow}{d\lambda} \simeq \frac{\mathcal{U}}{4\pi v_{C\downarrow}}, \tag{131}$$

where $\mathcal{U}$ is the inter-electron interaction term. This clearly shows that as $v_{C\uparrow}$ increases and $v_{C\downarrow}$ decreases with an increasing magnetic field, the renormalized barrier seen by the two spin species of electrons will be different. We also note that, just like the case of the infinite, homogeneous QW, a weak field of $h \ll E_{F1D}$ in our model of the QW does not give rise to the odd-even effect.

In summary, we can see that by turning on an external magnetic field in the QW system, the up and down spin electrons see different renormalized strengths of any barriers (or impurities) — this is the odd-even effect. We speculate on the possible use of this effect in creating a spin-valve using QW systems. The effective actions, their resonance symmetries as well as the temperature and length power-law corrections to the conductance in the various temperature regimes, however, still follow a pattern similar to that for a QW without a magnetic field.

6 Comparison with the Experiments

We now discuss the relevance of this model to many of the experiments that have been performed so far on quantum wire systems fabricated using cleaved-edge overgrowth as well as split-gate techniques. But before doing that, let us reiterate some well-known observations about the experimental system that we are trying to model here. In this system, the electrons enter the wire from the 2DEG reservoirs lying outside the wire with a Fermi energy E_F whose value (typically around $5 - 10meV$) is fixed by the parameters of the 2DEG. Within the quantum wire, the gate voltage produces a discrete set of sub-bands labeled by an integer s (see Fig. 2); let E_s denote the energies of the bottoms of these sub-bands. In a sufficiently long quantum wire, we expect E_s to be constant along the length of the wire provided we are not too close to either of the junctions. Thus an electron which has energy E_F and enters the sub-band s will have a wave number k_{Fs} inside the wire given by $k_{Fs}^2/2m = E_F - E_s$ and a velocity given by $v_{Fs} = k_{Fs}/m$ [21]. We know that if N of the $1D$ sub-bands lie below the 2DEG Fermi energy E_{F2D} (which itself at any finite temperature is surrounded by a small thermal spread), we will get N quantized steps in the conductance when the quantum wire is completely free of any impurities; this statement is true irrespective of the electron velocities, densities or how they interact among themselves while in the various channels [16, 17, 21]. Now, upon increasing the gate voltage V_G, one adds an energy eV_G to every electron in each of the 1D sub-bands in the quantum wire. This has the effect of pushing up each of the sub-bands by the same energy and can even de-populate the sub-bands by pushing them above E_{F2D} (see Fig. 2). Thus, changing the gate voltage decreases the electron density in the quantum wire and allows the transport process to take place through only a few channels, and in the extreme limit, only one channel, before cutting off the wire altogether by pushing all the 1D sub-bands above the E_{F2D} (this is called *pinch-off*). The conductance measurement which shows step quantization in terms of rises and plateaus can then be explained in the following way. Whenever, by decreasing the gate voltage V_G, the bottom one of the 1D sub-bands (which is initially well above E_{F2D}) first touches the top of the thermal spread just above E_{F2D}, that band starts filling up and so we can see a rise. Once the bottom of this sub-band crosses the bottom of the thermal spread just below E_{F2D}, the rise is topped off by a plateau which signals that another channel is fully open to electron transport between the two reservoirs (see Fig. 2). Some of the earliest experiments with quantum wires free of impurities did indeed reveal quantization of the conductance in integer steps of $2g_0$ [2].

But later Tarucha *et al* [3] performed experiments with wires of lengths of $2\mu m$ to $10\mu m$ fabricated using split-gate methods at temperatures from $0.3K$ to $1.1K$, and found deviations from the perfect quantization of the steps. Attempts were then made to explain these deviations as due to electron-electron interactions. Although, a clean TLL

wire between Fermi liquid leads would not lead to renormalization of the conductance quantization, several authors [18, 24, 27], showed that the presence of impurities in a TLL connected to Fermi leads would cause renormalization. However, they expected the renormalizations to be gate voltage dependent; this was indeed seen by Tarucha *et al* [3].

However, Yacoby *et al* [4] made the following surprising observation for a quantum wire $2\mu m$ long fabricated in cleaved-edge overgrowth systems: the dc conductance showed several nearly flat plateaus whose heights are uniformly renormalized from the ideal values of integer multiples of $2g_0$ for measurements made over a temperature range of $0.3 - 25K$. Similar observations were subsequently made in several experiments on quantum wires made using the split-gate technique [6, 7, 8, 12]. In all these experiments the step heights were increasingly renormalized as either the temperature was lowered (for a fixed length of quantum wire) or the length of the quantum wire was increased at a fixed temperature. Such renormalizations would require back-scattering of electrons. If these back-scatterings were due to impurities within the quantum wires, the conductance corrections would be gate voltage dependent as shown in our calculations. This can certainly not lead to flat conductance plateaus as seen in the experiments.

Our model, however, has contact regions independent of the gate voltage and has barriers at the contacts arising due to the changes in the nature of the electron-electron interactions and geometry. Thus, the back-scattering at these barriers is independent of gate voltage and the sub-band index (as can be seen in our results), and will lead to conductance plateaus which are flat as a function of gate voltage and uniform for all the sub-bands at the highest temperatures. We note that a recent experiment [9] on a quantum wire system similar to that used by Yacoby *et al* [4] revealed the existence of a region of length $2 - 6\mu m$ which lies in between the gated quantum wire region and the 2DEG reservoirs and gives rise to the back-scattering that causes the flat and uniform renormalization of the conductance of each sub-band. Such contact regions correspond to $T_d \sim 0.2 - 0.7K$. This is much less than most of the temperature range shown in Fig. 3 of Ref. [4]. The similar flat and uniform conductance corrections seen in the experiments of Refs. [6, 7, 8, 12] seem to suggest that their QW systems also include contact regions and have $T \gg T_d$.

Now, as explained earlier for a quantum wire system in which the contact length $d \ll l$, in the intermediate and low temperature regimes of $T_l \ll T \ll T_d$ and $T \ll T_l$, we know that the correct cutoffs for the RG procedure are T_d and T_l respectively; that is why the length power-laws of d and l appear in the conductance corrections in these two regimes besides the customary temperature power-law. We can clearly see that the inverse length scale d^{-1} (for the contact region) and l^{-1} (for the wire region) have similar power-laws to those obtained for the temperature. Thus, one can qualitatively understand the increase in the conductance with increasing temperature and its decrease as the length of the quantum

wire is increased. This has been observed by several groups [3, 4, 6, 8]. Furthermore, one recent experiment using a split-gate QW system [12] shows that the conductance of a $2\mu m$ long QW at $T = 1K$ shows flat, renormalized plateaus which are replaced by uneven conductance fluctuations at $T = 50mK$. However a different experiment [6] reveals that a QPC created using similar split-gate methods shows plateaus which are hardly renormalized at higher temperatures, and no conductance fluctuations are seen at lower temperatures. This can also be understood from our model: the conductance corrections due the junction barriers for a quantum wire are gate voltage independent at higher temperatures, but are dependent on it at lower temperatures. For the experiment in Ref. [12], $T_l = 0.4K >> T = 50mK$. Hence, resonance effects are expected at these temperatures. This is in contrast to the conductance corrections for a QPC which are gate voltage independent at all temperatures. In fact, if the quantum wire samples of Yacoby *et al* have contact regions as long as $2 - 6\mu m$ (as found by the authors of Ref. [9] on similar samples), this would suggest that their $2\mu m$ long wire is actually closer to a quantum point contact. This would help explain the flatness of the renormalizations seen over a wide temperature range of $0.3 - 25K$.

We now discuss our attempt to quantitatively understand the variation of conductance against temperature as given in the inset of Fig. 3 of the work of Yacoby *et al* [4]. The conductance given there is measured at a fixed value of the gate voltage on the plateau of the first sub-band (i.e., close to $2g_0$). We find that the conductance correction versus temperature variation found by them (i.e., $\delta g \equiv 2g_0 - g$ vs. T) is best fitted by a function of the form

$$\delta g = -0.3512\ T^{-0.1058-0.0345T} \tag{132}$$

as shown in Fig. 3. We find that the goodness of this fit is given by the correlation coefficient $R^2 = 0.9955$. Clearly, this expression for the conductance corrections does not match the simple form $\delta g \sim T^{-\alpha}$ given in Sec. 4 for the QW or QPC systems. The presence of the T dependent piece in the exponent implies that our model is only qualitatively correct. Several factors could be important in determining this complicated temperature dependent power-law. Some of these are:

- a more extended transition region between the leads and the contacts in which the parameters K and v vary smoothly as a function of x,
- more extended junction barriers lying within the contacts rather than the local δ-function barriers that we have studied, and
- the possibility of the electron-electron interactions having a finite range instead of the short-ranged interactions that we have used to study our TLL systems.

A detailed quantitative comparison of our model with the experiments would, therefore, need a more sophisticated treatment taking these factors into consideration. We should emphasize here that a temperature and length dependence of the conductance correction of the form that we have obtained (decreasing at high temperatures or short lengths) is a nontrivial effect of the electron interactions, and our simple model has already captured this qualitatively. A non-interacting theory does not have temperature or length dependences of this kind.

We now discuss the important experimental finding of Liang *et al* [7] of the odd-even effect in the transport of electrons through a quantum wire in the presence of a magnetic field. Liang *et al* find that as they turn up the external magnetic field (kept in plane and aligned along the direction of the channel) from 0 to $11T$, the increasing magnetic field expectedly lifts the spin degeneracy and splits each conductance step into two steps, with the heights of both being less than g_0. Furthermore, at a magnetic field strength of $11T$, they find that the difference between the conductance of successive pairs of spin-split sub-bands alternates. This shows that the conductance of the odd numbered spin-split sub-bands containing the moments aligned with the magnetic field undergoes little renormalization (i.e., is close to g_0 in their Fig. 4), while the conductance of the even numbered spin-split sub-bands containing the moments anti-aligned with the magnetic field undergoes a large renormalization correction; their Fig. 4 indicates a correction as large as $0.3g_0$. As discussed earlier, this phenomenon can be simply understood as the aligned moments seeing a much weaker barrier and the anti-aligned moments seeing a much stronger barrier. This is due to the Zeeman splitting of the Fermi levels of the up and down spin electrons and their interactions with each other. Since the difference in renormalizations between the aligned and anti-aligned electrons occur for all magnetic fields (i.e., even when the up and down sub-bands are not spin-split), we suggest the following possibility. One can artificially enhance the barrier strengths so that the difference in renormalizations of the up and down spins can be made substantial at moderate magnetic fields. More importantly, we can vary the gate voltage so as to tune the spin polarization with greater transmission to resonance. This would mean that at these values of the magnetic field and gate voltage, transmission of one of the polarizations is completely suppressed and the other one greatly enhanced. This leads us to the possibility of creating a spin-valve at moderate magnetic fields.

Finally, we comment on a new set of experiments [10, 11] which have used scanning probe microscopy techniques to study transport through QPCs and propose a test for our model based on such a study. In these experiments, a negatively charged atomic force microscope tip is held at a distance of $100 - 150nm$ above the 2DEG gas on which the QPC is created via split-gate methods. A capacitive coupling between the 2DEG and the tip reduces the density of the 2DEG in a small spot directly beneath the tip,

thereby creating a small depletion region (negatively charged "bubble") which can back-scatter electrons approaching it. The tip then scans the surface of the 2DEG reservoir into which the electrons are entering after traveling through the QPC, and the two-probe conductance is measured. This allows one to "image" the electron current flowing out from the QPC. Topinka *et al* [10] have made such measurements at a temperature of $T = 1.7K$ and find that the electrons flow out into the 2DEG reservoir in streaks from each sub-band. The number and nature of the streaks is governed by the electron wave function in each sub-band caused by the quantization due to the confinement in the transverse direction. They find that the electron flow is coherent along these streaks quite far from the QPC mouth where they finally disperse into the 2DEG. Furthermore, they find that placing the depletion bubble in the path of a particular streak (at a distance of about $0.3 - 0.5\mu m$ from the mouth of the QPC) gives rise to a flat, renormalized plateau only for the particular sub-band from which it is emanating, while the other sub-bands give the universal conductance value of $2g_0$. This tells us that the effect of the gate voltage must vanish quickly since it is not felt beyond distances as short as $0.3 - 0.5\mu m$ from the mouth of the QPC. Crook *et al* [11] find a series of peaks and troughs upon measuring the differential conductance dg/dV_G versus the gate voltage V_G (which are caused by the step rises and plateaus for each sub-band respectively) while scanning the tip through the QPC. Their finding that the troughs do not fall to zero indicate that the conductance corrections caused by the depletion bubble (when placed within the QPC) is gate voltage dependent as would have been expected.

Now, the availability of the tip generated depletion bubble as a controlled barrier to the flow of electrons through the QPC also suggests a possible use of scanning probe microscopy techniques to test the predictions of our model in a quantitative fashion. This would require the gate voltage to be first fixed such that only the lowest sub-band is fully open to the flow of electron current, and then the depletion bubble to be placed somewhere on a streak emanating from this lowest sub-band at a distance from the QPC mouth; the conductance can then be measured by changing the gate voltage but holding the temperature fixed. The nature of the conductance versus gate voltage curve will tell us whether the gate voltage does or does not have any effect on the electrons on the streak at that distance from the mouth of the QPC. Furthermore, the gate voltage can then be held fixed somewhere on a plateau and the conductance measured as the temperature is varied. The form of the conductance corrections versus temperature can then be obtained. This entire chain of measurements can then be repeated after taking the depletion bubble closer to the QPC mouth and into the QPC in a series of steps. Such a series of measurements would help answer questions about where the conductance corrections start becoming dependent on the gate voltage as well as how the conductance corrections vary with temperature when a barrier is placed within the QPC or away from the QPC. Such experiments could also be carried out with longer QWs to check the length

dependences of the conductance corrections.

7 Summary and Outlook

The main idea in this paper is to introduce a model which explicitly describes the regions in between the quantum wire and the 2DEG reservoirs as interacting 1D systems which are independent of the density of electrons in the quantum wire. We show that the difference in the strengths of the interactions in the different regions leads to local junction barriers between the regions; the barriers simulate the effects of the imperfect coupling between the 2DEG and the quantum wire. Our model leads to the following results for wires with no impurities, all of which are in agreement with a large body of experimental observations.

- Flat (independent of gate voltage) and uniform (for all the sub-bands) renormalizations of the quantized conductance plateaus.
- The renormalizations increase as the temperature is lowered or the length of the quantum wire is increased.
- At still lower temperatures, the flatness of the plateaus disappears and oscillatory features in the conductance can be observed which we interpret as resonant transmission through the quantum wire.
- In the presence of a magnetic field, an odd-even effect is found in the conductance of alternate spin-split sub-bands. This effect may be used to construct a spin-valve, which allows only electrons with one particular spin to transmit through the wire even if the magnetic field is not high enough to completely spin-split the sub-bands.

For quantum wires with impurities, which are either intrinsic or externally imposed as finger gates, the conductance corrections are always gate voltage dependent and therefore, are neither flat nor sub-band independent.

Some interesting questions for future studies include the following. A quantitative fit to the conductance corrections as a function of the temperature and wire length still remains to be done. This would require an even more realistic modeling of the quantum wire system (including some of the features itemized in the previous section) as well as more experimental data. Theoretical studies at finite frequencies and finite external voltages across the quantum wire also need to be pursued. Finally, one needs to understand several features which are observed on the rise between two successive plateaus, such as the "0.7 effect" mentioned in the introduction, the observation of continuous oscillations as a function of the gate voltage upon introducing finger gate barriers [29], and the fixed

point that exists on the rise as the temperature is varied [30]. For all of these, one needs to study the model when some sub-band is partially opened.

Acknowledgments

SL thanks I. Safi for useful correspondence. DS thanks the Council of Scientific and Industrial Research, India for financial support through grant No. 03(0911)/00/EMR-II.

A Effective action for spinless fermions

In this Appendix, we will obtain explicitly the S_0 part of the effective action in terms of the fields $\phi_i, i = 1, ..4$, at the junctions $x = 0, d, l + d$ and $x = l + 2d = L$ for the K_L-K_C-K_W-K_C-K_L model described by the action in Eq. (12) by integrating out all degrees of freedom except at the positions of the junctions. We will also give the effective action of the simpler model K_L-K_W-K_L for comparison, since they have also not been explicitly given anywhere.

We first start with the simpler K_L-K_W-K_C model, which is defined as a length L quantum wire with interaction parameter K_W between $x = 0$ and $x = L$, and with leads defined by $K_L = 1$ for $x < 0$ and $x > L$, described by the Lagrangian

$$\mathcal{L} = \int_{-\infty}^{0} dx \mathcal{L}_1 + \int_{0}^{L} dx \mathcal{L}_2 + \int_{L}^{\infty} dx \mathcal{L}_1, \tag{133}$$

where

$$\begin{aligned} \mathcal{L}_1 &= \frac{1}{2K_L v_L}(\partial_\tau \phi)^2 + \frac{v_L}{2K_L}(\partial_x \phi)^2, \\ \text{and} \quad \mathcal{L}_2 &= \frac{1}{2K_W v_W}(\partial_\tau \phi)^2 + \frac{v_W}{2K_W}(\partial_x \phi)^2. \end{aligned} \tag{134}$$

to set the notation. There are three ways to derive the effective action. We can (a) integrate out the fields at all points in space except at $x = 0$ and L, or (b) find the solution of the equations of motion in terms of the above two fields and then compute the action from that solution, or (c) compute the Green's function $G_{\bar{\omega}}(x, x')$, set x, x' equal to 0 or L, and invert G to get S_{eff}. All the methods produce the same result since the original action is purely quadratic. We will use the second method here because it is technically simpler.

As in other sections, we will work with the Euclidean time action for convenience. If all the fields have a time dependence of the form $\exp(-i\bar{\omega}_n \tau)$, then normalizability of the

solutions imply that they should decay exponentially at $x \to \pm\infty$. We assume that the solution of the equation of motion has the following forms in the three regions,

$$\begin{aligned}\tilde{\phi}(x,\bar{\omega}_n) &= \tilde{\phi}(0,\bar{\omega}_n)e^{-i\bar{\omega}_n\tau+|\bar{\omega}_n|x/v_L}, \quad x<0 \\ &= e^{-i\bar{\omega}_n\tau}(\tilde{\theta}_1(\bar{\omega}_n)e^{|\bar{\omega}_n|x/v_W}+\tilde{\theta}_2(\bar{\omega}_n)e^{-\bar{\omega}_n x/v_W}), \quad 0<x<L \\ &= \tilde{\phi}(L,\bar{\omega}_n)e^{-i\bar{\omega}_n\tau+|\bar{\omega}_n|(L-x)/v_L}, \quad x>L\ . \end{aligned} \tag{135}$$

Matching solutions at the boundaries $x=0$ and $x=L$ to eliminate $\tilde{\theta}_i(\bar{\omega}_n)$, and using this solution in the effective action and carrying out the spatial integration, we obtain the action

$$\begin{aligned}S_0 &= \frac{1}{2K_L}\sum_{\bar{\omega}_n}|\bar{\omega}_n|(\tilde{\phi}_1^2+\tilde{\phi}_2^2)+\frac{1}{2K_W}\sum_{\bar{\omega}_n}\frac{|\bar{\omega}_n|}{e^{k_{nW}L}-e^{-k_{nW}L}}\times \\ &\qquad [(e^{k_{nW}L}+e^{-k_{nW}L})(\tilde{\phi}_1^2+\tilde{\phi}_2^2)-4\tilde{\phi}_1\tilde{\phi}_2],\end{aligned} \tag{136}$$

where $\tilde{\phi}_1 \equiv \tilde{\phi}(0,\bar{\omega}_n)$ and $\tilde{\phi}_2 \equiv \tilde{\phi}(L,\bar{\omega}_n)$ and k_{nW} and k_{nL} are defined as $|\bar{\omega}_n|/v_W$ and $|\bar{\omega}_n|/v_L$ respectively. In the limit $\bar{\omega}_n \gg v_L/L, v_W/L$, we get the high frequency effective action

$$S_{high} = \frac{K_L+K_W}{2K_LK_W}\sum_{\bar{\omega}_n}|\bar{\omega}_n|(\tilde{\phi}_1^2+\tilde{\phi}_2^2)\ , \tag{137}$$

where the two junctions are decoupled as expected. In the low frequency limit $\bar{\omega}_n \ll v_L/L, v_W/L$, we get

$$S_{low} = \frac{1}{2K_L}\sum_{\bar{\omega}_n}|\bar{\omega}_n|(\tilde{\phi}_1^2+\tilde{\phi}_2^2)+\frac{U_W}{2}\sum_{\bar{\omega}_n}|\bar{\omega}_n|(\tilde{\phi}_1-\tilde{\phi}_2)^2\ , \tag{138}$$

where $U_W = v_W/K_WL$.

Using the same method as above, we can also obtain the full effective action for the K_L-K_C-K_W-K_C-K_L model in terms of the fields at the four junctions $\phi_i, i=1,..4$, where $\tilde{\phi}(0,\bar{\omega}_n)=\tilde{\phi}_1(\bar{\omega}_n)\equiv\tilde{\phi}_1$, $\tilde{\phi}(d,\bar{\omega}_n)\equiv\tilde{\phi}_2$, $\tilde{\phi}(l+d,\bar{\omega}_n)\equiv\tilde{\phi}_3$ and $\tilde{\phi}(L=l+2d,\bar{\omega}_n)\equiv\tilde{\phi}_4$. The solutions in the five regions can be written as

$$\begin{aligned}\tilde{\phi}(x,\bar{\omega}_n) &= \tilde{\phi}_1 e^{k_{nL}x}, \quad x<0 \\ &= Be^{k_{nC}x}+Ce^{-k_{nC}x}, \quad 0<x<d \\ &= De^{k_{nW}x}+Ee^{-k_{nW}x}, \quad d<x<l+d \\ &= Fe^{k_{nC}x}+Ge^{-k_{nC}x}, \quad l+d<x<L \\ &= \tilde{\phi}_4 e^{k_{nL}(L-x)}, \quad x<0\ . \end{aligned} \tag{139}$$

where by matching the solutions at $x=0,d,l+d$ and L, we can obtain the functions of $\bar{\omega}_n$, B,C,D,E,F and G in terms of the $\tilde{\phi}_i, i=1...4$, and k_{nC} is defined as $k_{nC}=|\bar{\omega}_n|/v_C$.

Substituting this solution in the action and integrating over all space, we get the effective action

$$\begin{aligned} S_{eff} &= \sum_{\bar{\omega}_n} \{ \frac{1}{2K_L} |\bar{\omega}_n| (\tilde{\phi}_1^2 + \tilde{\phi}_4^2) \\ &+ \frac{1}{2K_C} |\bar{\omega}_n| [(B^2 + G^2 e^{-2k_n L})(e^{2k_n d} - 1) + (C^2 + F^2 e^{2k_n L})(1 - e^{-2k_n d})] \\ &+ \frac{1}{2K_W} [|\bar{\omega}_n| [D^2 (e^{2k_n (L-d)} - e^{2k_n d}) - E^2 (e^{-2k_n (L-d)} - e^{-2k_n d})]] \} \ , \end{aligned} \tag{140}$$

with

$$\begin{aligned} B &= \frac{\tilde{\phi}_2 - \tilde{\phi}_1 e^{-k_{nC} d}}{e^{k_{nC} d} - e^{-k_{nC} d}}, & C &= \frac{\tilde{\phi}_1 e^{k_{nC} d} - \tilde{\phi}_2}{e^{k_{nC} d} - e^{-k_{nC} d}} \\ D &= \frac{\tilde{\phi}_3 - \tilde{\phi}_2 e^{-k_{nW} l}}{e^{k_{nC} d} (e^{k_{nW} l} - e^{-k_{nW} l})}, & E &= \frac{\tilde{\phi}_2 e^{k_{nW} l} - \tilde{\phi}_2}{e^{-k_{nC} d} (e^{k_{nW} l} - e^{-k_{nW} l})} \\ F &= \frac{\tilde{\phi}_4 - \tilde{\phi}_3 e^{-k_{nC} d}}{e^{k_{nC} d + k_{nW} l} (e^{k_{nC} d} - e^{-k_{nC} d})}, & G &= \frac{\tilde{\phi}_3 e^{k_{nC} d} - \tilde{\phi}_4}{e^{-k_{nC} d - k_{nW} l} (e^{k_{nC} d} - e^{-k_{nC} d})} \ . \end{aligned} \tag{141}$$

The action finally simplifies to

$$\begin{aligned} S_{eff} &= \frac{1}{2K_L} \sum_{\bar{\omega}_n} |\bar{\omega}_n| (\tilde{\phi}_1^2 + \tilde{\phi}_4^2) \\ &+ \frac{1}{2K_C} \sum_{\bar{\omega}_n} \frac{|\bar{\omega}_n|}{e^{k_{nC} d} - e^{-k_{nC} d}} [(e^{k_{nC} d} + e^{-k_{nC} d})(\tilde{\phi}_1^2 + \tilde{\phi}_2^2 + \tilde{\phi}_3^2 + \tilde{\phi}_4^2) - 4\tilde{\phi}_1 \tilde{\phi}_2 - 4\tilde{\phi}_3 \tilde{\phi}_4] \\ &+ \frac{1}{2K_W} \sum_{\bar{\omega}_n} \frac{|\bar{\omega}_n|}{e^{k_{nW} l} - e^{-k_{nW} l}} [(e^{k_{nW} l} + e^{-k_{nW} l})(\tilde{\phi}_2^2 + \tilde{\phi}_3^2) - 4\tilde{\phi}_2 \tilde{\phi}_3] \ , \end{aligned} \tag{142}$$

where $\tilde{\phi}_1 \equiv \tilde{\phi}(0, \bar{\omega}_n)$ and $\tilde{\phi}_2 \equiv \tilde{\phi}(L, \bar{\omega}_n)$. The high and low frequency limits of this effective action have been used in Sec. 3, to compute the finite temperature and finite length corrections off-resonance.

B Effective action for spinful fermions

In this section, we will explicitly compute the effective action for spinful fermions in the K_L-K_C-K_W-K_C-K_L model. Although, the method followed is exactly the same as that in the previous section for spinless fermions, we do it explicitly because there are a few points where the inclusion of spin makes a difference.

The effective action for spinful fermions is normally computed in terms of the 'charge' and 'spin' field variables defined as $\phi_\rho = (\phi_\uparrow + \phi_\downarrow)/\sqrt{2}$ and $\phi_\sigma = (\phi_\uparrow - \phi_\downarrow)/\sqrt{2}$ because in the presence of interactions, the spin $\uparrow$ and $\downarrow$ fermions are mixed (remember the Hubbard term $\mathcal{U}\sum_i n_{i\uparrow}n_{i\downarrow}$). Here, in our model with contacts, the interaction term $\mathcal{U}$ is different in the contact region and in the wire region. But since the linear combination that diagonalizes the interaction is independent of the value of $\mathcal{U}$, the action in terms of the ϕ_ρ and ϕ_σ fields are decoupled. In the presence of a magnetic field, in the next Appendix, we will see that the action continues to be diagonalizable; however, the diagonal fields are defined in terms of mixing angles which explicitly depend on $\mathcal{U}$ and the magnetic field and hence are different in the leads, the contacts and the wire.

The starting action for the spinful fermions is given in Eqs. (12) and (13) in the text in terms of the charge and spin fields. As in the earlier Appendix, we will obtain the solution of the equations of motion in terms of the eight fields $\tilde{\phi}_{ia}, i = 1...4, a = \rho, \sigma$ defined to be at the positions $x = 0, d, l + d$ and $L = l + 2d$ and then compute the effective action from that solution. We assume that the solutions in the five regions can be written as

$$\begin{aligned}
\tilde{\phi}_a(x,\bar{\omega}_n) &= \tilde{\phi}_{1a}e^{k_{nLa}x}, \quad x < 0 \\
&= B_a e^{k_{nCa}x} + C_a e^{-k_{nCa}x}, \quad 0 < x < d \\
&= D_a e^{k_{nWa}x} + E_a e^{-k_{nWa}x}, \quad d < x < l + d \\
&= F_a e^{k_{nCa}x} + G_a e^{-k_{nCa}x}, \quad l + d < x < L \\
&= \tilde{\phi}_{4a}e^{k_{nL}(L-x)}, \quad x < 0 \ . \qquad (143)
\end{aligned}$$

and as before, the coefficients, B_a, C_a, D_a, E_a, F_a and G_a can be found in terms of the $\tilde{\phi}_{ia}, i = 1...4, a = \rho, \sigma$ by matching the solutions at $x = 0, d, l + d$ and L. Note that k_{nWa}, k_{nCa} and k_{nL} are defined as $|\bar{\omega}_n|/v_{Wa}$, $|\bar{\omega}_n|/v_{Ca}$ and $|\bar{\omega}_n|/v_{La}$ respectively. Substituting this solution in the action and integrating over all space, we get the effective action as

$$\begin{aligned}
S &= \sum_{a=\rho,\sigma}\{\frac{1}{2K_{La}}\sum_{\bar{\omega}_n}|\bar{\omega}_n|(\tilde{\phi}_{1a}^2 + \tilde{\phi}_{4a}^2) + \frac{1}{2K_{Ca}}\sum_{\bar{\omega}_n}\frac{|\bar{\omega}_n|}{e^{k_{nCa}d} - e^{-k_{nCa}d}} \times \\
&\qquad [(e^{k_{nCa}d} + e^{-k_{nCa}d})(\tilde{\phi}_{1a}^2 + \tilde{\phi}_{2a}^2 + \tilde{\phi}_{3a}^2 + \tilde{\phi}_{4a}^2) - 4\tilde{\phi}_{1a}\tilde{\phi}_{2a} - 4\tilde{\phi}_{3a}\tilde{\phi}_{4a}] \\
&+ \frac{1}{2K_{Wa}}\sum_{\bar{\omega}_n}\frac{|\bar{\omega}_n|}{e^{k_{nWa}l} - e^{-k_{nWa}l}}[(e^{k_{nWa}l} + e^{-k_{nWa}l})(\tilde{\phi}_{2a}^2 + \tilde{\phi}_{3a}^2) - 4\tilde{\phi}_{2a}\tilde{\phi}_{3a}]\}. \qquad (144)
\end{aligned}$$

The high and low frequency limits of this effective action have been used in Sec. 3, to discuss the various resonances that are possible in the low temperature limit and to explicitly compute the off-resonance corrections to the conductances at finite temperatures and for finite length wires.

C Effective action for spinful electrons in the presence of a magnetic field

We present here the calculation for the effective action for spinful fermions in a magnetic field when the mixing angle γ is the same in both the contacts as well as the QW, i.e., the short ranged electron-electron interaction $\mathcal{U}$ is equal in all the three TLLs. We start with the action given in Eq. (102) in Sec. 5 and will now integrate out the fields at all points except at the four junctions as these will be the sites for the two outer barriers while the two inner junctions are the ends of the region to which the gate voltage couples. Thus, we write down the equations of motion in each of the five regions and solve them. If all the fields have a time dependence of the form $\exp(-i\bar{\omega}_n\tau)$, then normalizability of the solutions imply that they should decay exponentially at $x \to \pm\infty$. The general solution is given by

$$\begin{aligned}
\tilde{\phi}_\uparrow(x) &= A_\uparrow e^{k_\uparrow x}, \quad \tilde{\phi}_\downarrow(x) = A_\downarrow e^{k_\downarrow x}, \quad x < 0 \\
\tilde{\phi}_\pm(x) &= B_\pm e^{k_\pm x} + C_\pm e^{-k_\pm x}, \quad 0 < x < d \\
\tilde{\phi}_\pm(x) &= D_\pm e^{\tilde{k}_\pm x} + E_\pm e^{-\tilde{k}_\pm x}, \quad d < x < l + d \\
\tilde{\phi}_\pm(x) &= F_\pm e^{k_\pm x} + G_\pm e^{-k_\pm x}, \quad l + d < x < l + 2d \\
\tilde{\phi}_\uparrow(x) &= H_\uparrow e^{k_\uparrow x}, \quad \tilde{\phi}_\downarrow = H_\downarrow e^{k_\downarrow x}, \quad x < 0 \ , \qquad (145)
\end{aligned}$$

where we have defined $\tilde{k}_\pm = |\bar{\omega}_n|/v_{W\pm}$, $k_\pm = |\bar{\omega}_n|/v_{C\pm}$, $k_\uparrow = |\bar{\omega}_n|/v_{F\uparrow}$ and $k_\downarrow = |\bar{\omega}_n|/v_{F\downarrow}$.

We now solve for the coefficients $A, ..., H$ in Eq. (145) by matching the fields $\tilde{\phi}_\uparrow$ and the $\tilde{\phi}_\downarrow$ at the four junctions. At this point, we make the simplifying assumption that the mixing angles γ_C and γ_W (defined as in Eqs. (90) and (91)) in the contact and wire regions are equal to each other, $\gamma_C = \gamma_W = \gamma$. This implies that $\tilde{\phi}_{W\pm} = \sqrt{\frac{K_{W\pm}v_{W\pm}}{K_{C\pm}v_{C\pm}}}\tilde{\phi}_{C\pm}$ at $x = d$ and $x = l + d$. We find that the coefficients are given by

$$\begin{aligned}
A_\uparrow &= \tilde{\phi}_{1\uparrow}, \quad A_\downarrow = \tilde{\phi}_{1\downarrow} \\
B_\pm &= \frac{\tilde{\phi}_{2\pm} - \tilde{\phi}_{1\pm}e^{-k_\pm d}}{D_{C\pm}} \\
C_\pm &= -\frac{\tilde{\phi}_{2\pm} + \tilde{\phi}_{1\pm}e^{k_\pm d}}{D_{C\pm}} \\
D_\pm &= \sqrt{\frac{K_{W\pm}v_{W\pm}}{K_{C\pm}v_{C\pm}}}e^{-\tilde{k}_\pm d}\ \frac{(-\tilde{\phi}_{2\pm}e^{-\tilde{k}_\pm l} + \tilde{\phi}_{3\pm})}{D_{W\pm}} \\
E_\pm &= \sqrt{\frac{K_{W\pm}v_{W\pm}}{K_{C\pm}v_{C\pm}}}e^{\tilde{k}_\pm d}\ \frac{(\tilde{\phi}_{2\pm}e^{\tilde{k}_\pm l} - \tilde{\phi}_{3\pm})}{D_{W\pm}}
\end{aligned}$$

$$
\begin{aligned}
F_{\pm} &= -\frac{\tilde{\phi}_{3\pm}e^{-k_{\pm}(l+2d)} - \tilde{\phi}_{4\pm}e^{-k_{\pm}d}}{D_{C\pm}} \\
G_{\pm} &= \frac{\tilde{\phi}_{3\pm}e^{k_{\pm}(l+2d)} - \tilde{\phi}_{4\pm}e^{k_{\pm}d}}{D_{C\pm}} \\
H_{\uparrow} &= \tilde{\phi}_{4\uparrow}e^{k_{\uparrow}(l+2d)}, \quad H_{\downarrow} = \tilde{\phi}_{4\downarrow}e^{k_{\downarrow}(l+2d)} \ ,
\end{aligned} \tag{146}
$$

where

$$
\begin{aligned}
D_{C\pm} &= e^{k_{\pm}d} - e^{-k_{\pm}d} \\
\text{and} \quad D_{W\pm} &= e^{\tilde{k}_{\pm}l} - e^{-\tilde{k}_{\pm}l} \ .
\end{aligned} \tag{147}
$$

Then using the relations written down in Eq. (90) connecting the $\phi_{\pm}$ and $\phi_{\uparrow,\downarrow}$ fields, we find that the effective Lagrangian density is given by

$$
\begin{aligned}
\mathcal{L} = \quad & \frac{|\bar{\omega}_n|}{2K_L}(\tilde{\phi}_{1\uparrow}^2 + \tilde{\phi}_{1\downarrow}^2\tilde{\phi}_{4\uparrow}^2 + \tilde{\phi}_{4\downarrow}^2) \\
& + \frac{|\bar{\omega}_n|}{2}[(p^2\frac{N_{C+}}{K_{C+}D_{C+}} + r^2\frac{N_{C-}}{K_{C-}D_{C-}})(\tilde{\phi}_{1\uparrow}^2 + \tilde{\phi}_{2\uparrow}^2 + \tilde{\phi}_{3\uparrow}^2 + \tilde{\phi}_{4\uparrow}^2) \\
& + (q^2\frac{N_{C+}}{K_{C+}D_{C+}} + s^2\frac{N_{C-}}{K_{C-}D_{C-}})(\tilde{\phi}_{1\downarrow}^2 + \tilde{\phi}_{2\downarrow}^2 + \tilde{\phi}_{3\downarrow}^2 + \tilde{\phi}_{4\downarrow}^2) \\
& - 4(\frac{p^2}{K_{C+}D_{C+}} + \frac{r^2}{K_{C-}D_{C-}})(\tilde{\phi}_{1\uparrow}\tilde{\phi}_{2\uparrow} + \tilde{\phi}_{3\uparrow}\tilde{\phi}_{4\uparrow}) \\
& - 4(\frac{q^2}{K_{C+}D_{C+}} + \frac{s^2}{K_{C-}D_{C-}})(\tilde{\phi}_{1\downarrow}\tilde{\phi}_{2\downarrow} + \tilde{\phi}_{3\downarrow}\tilde{\phi}_{4\downarrow})] \\
& + |\bar{\omega}_n|[(\frac{pqN_{C+}}{K_{C+}D_{C+}} + \frac{rsN_{C-}}{K_{C-}D_{C-}})(\tilde{\phi}_{1\uparrow}\tilde{\phi}_{1\downarrow} + \tilde{\phi}_{2\uparrow}\tilde{\phi}_{2\downarrow} + \tilde{\phi}_{3\uparrow}\tilde{\phi}_{3\downarrow} + \tilde{\phi}_{4\uparrow}\tilde{\phi}_{4\downarrow}) \\
& - 2(\frac{pq}{K_{C+}D_{C+}} + \frac{rs}{K_{C-}D_{C-}})(\tilde{\phi}_{1\uparrow}\tilde{\phi}_{2\downarrow} + \tilde{\phi}_{1\downarrow}\tilde{\phi}_{2\uparrow} + \tilde{\phi}_{3\uparrow}\tilde{\phi}_{4\downarrow} + \tilde{\phi}_{3\downarrow}\tilde{\phi}_{4\uparrow})] \\
& + \frac{|\bar{\omega}_n|}{2}[(p^2\frac{N_{W+}}{K_{W+}D_{W+}} + r^2\frac{N_{W-}}{K_{W-}D_{W-}})(\tilde{\phi}_{2\uparrow}^2 + \tilde{\phi}_{3\uparrow}^2) \\
& + (q^2\frac{N_{W+}}{K_{W+}D_{W+}} + s^2\frac{N_{W-}}{K_{W-}D_{W-}})(\tilde{\phi}_{2\downarrow}^2 + \tilde{\phi}_{3\downarrow}^2) \\
& - 4(\frac{p^2}{K_{W+}D_{W+}} + \frac{r^2}{K_{W-}D_{W-}})\tilde{\phi}_{2\uparrow}\tilde{\phi}_{3\uparrow} \\
& - 4(\frac{q^2}{K_{W+}D_{W+}} + \frac{s^2}{K_{W-}D_{W-}})\tilde{\phi}_{2\downarrow}\tilde{\phi}_{3\downarrow}] \\
& + |\bar{\omega}_n|[(\frac{pqN_{W+}}{K_{W+}D_{W+}} + \frac{rsN_{W-}}{K_{W-}D_{W-}})(\tilde{\phi}_{2\uparrow}\tilde{\phi}_{2\downarrow} + \tilde{\phi}_{3\uparrow}\tilde{\phi}_{3\downarrow})
\end{aligned}
$$

$$-2(\frac{pq}{K_{W+}D_{W+}} + \frac{rs}{K_{W-}D_{W-}})(\tilde{\phi}_{2\uparrow}\tilde{\phi}_{3\downarrow} + \tilde{\phi}_{2\downarrow}\tilde{\phi}_{3\uparrow})], \tag{148}$$

where

$$\begin{aligned} N_{C\pm} &= e^{k_\pm d} + e^{-k_\pm d}\ , \\ N_{W\pm} &= e^{\tilde{k}_\pm l} + e^{-\tilde{k}_\pm l}\ , \end{aligned} \tag{149}$$

and $D_{C\pm}, D_{W\pm}, k_\pm$ and $\tilde{k}_\pm$ have already been defined above.

D Calculation of the Green's function in our model for the Quantum Wire

Here, we will present a calculation of the Green's function for the bosonic excitations in the model that we have presented for the quantum wire system of spinless fermions. The method we follow is along the lines of the calculation presented by Maslov and Stone [17]. We will study the case when there are no barriers present anywhere in the system. Then, we see that the Euclidean action S_E in all the five distinct TLL regions in our model (Fermi lead, contact, QW, contact and Fermi lead) is given by

$$S_E = \frac{1}{2}\int_0^\beta d\tau \int_{-\infty}^{\infty}[\frac{1}{K(x)v(x)}(\partial_\tau\phi)^2 + \frac{v(x)}{K(x)}(\partial_x\phi)^2], \tag{150}$$

with $K(x) = K_L, v(x) = v_L$ in the first and fifth (Fermi lead) regions, $K(x) = K_C, v(x) = v_C$ in the second and fourth (contact) regions and $K(x) = K_W, v(x) = v_W$ in the third (QW) region. Then, defining the two-point bosonic Green's function/propagator (in Euclidean time τ) as

$$G(x, x', \tau) =< T_\tau\phi(x, \tau)\phi(x', 0) >, \tag{151}$$

it can be shown that the equation satisfied by the Fourier transform of the above Green's function $G_{\bar{\omega}}(x, x')$ is

$$\{-\partial_x(\frac{v(x)}{K(x)}\partial_x) + \frac{1}{K(x)v(x)}\bar{\omega}^2\}G_{\bar{\omega}}(x, x') = \delta(x - x'). \tag{152}$$

We now have to solve the above equation to obtain a functional form for $G_{\bar{\omega}}(x, x')$. We know that the interaction parameter K and the velocity v change abruptly at each of the junctions and that the two Fermi leads are semi-infinite in length (i.e. $G_{\bar{\omega}}(x, x')$ must decay to zero as $x \to \pm\infty$). As we are interested in finding the one-point Green's function at a point in the left contact, we will choose x' to lie between 0 (the left lead-contact junction) and d (the left contact-QW junction). Furthermore, we know that the

Green's function $G_{\bar{\omega}}(x,x')$ must satisfy the following boundary conditions: (a) $G_{\bar{\omega}}(x,x')$ must be continuous at $x=0,x',d,l+d$ and $l+2d$ (b) $(\frac{v(x)}{K(x)})\partial_x G_{\bar{\omega}}(x,x')$ must be continuous at $x=0,d,l+d$ and $l+2d$ and

$$-\frac{v(x)}{K(x)}\partial_x G_{\bar{\omega}}(x,x')|_{x=x'-0}^{x=x'+0}=1, \tag{153}$$

i.e., $(\frac{v(x)}{K(x)})\partial_x G_{\bar{\omega}}(x,x')$ undergoes a jump of unity at $x=x'$. It is then easily seen that the solution for $G_{\bar{\omega}}(x,x')$ is of the form

$$\begin{aligned}
G_{\bar{\omega}}(x,x') &= Ae^{|\bar{\omega}|x/v_L} && \text{for } x\le 0\\
&= Be^{|\bar{\omega}|x/v_C}+Ce^{-|\bar{\omega}|x/v_C} && \text{for } 0<x\le x'\\
&= De^{|\bar{\omega}|x/v_C}+Ee^{-|\bar{\omega}|x/v_C} && \text{for } x'<x\le d\\
&= Fe^{|\bar{\omega}|x/v_C}+Ge^{-|\bar{\omega}|x/v_C} && \text{for } d<x\le l+d\\
&= He^{|\bar{\omega}|x/v_C}+Ie^{-|\bar{\omega}|x/v_C} && \text{for } l+d<x\le l+2d\\
&= Je^{-|\bar{\omega}|x/v_C} && \text{for } l+2d<x\ .
\end{aligned} \tag{154}$$

The coefficients $A,B,\ldots,J$ are found by matching the boundary conditions. To begin with, it is worth noting that in the dc limit of $\bar{\omega}\to 0$, we find that

$$A=B+C=D+E=F+G=H+I=J=\frac{K_L}{2|\bar{\omega}|}, \tag{155}$$

which gives the dc conductance to be

$$g=\frac{2e^2}{h}K_L=2g_0K_L. \tag{156}$$

This gives the perfect quantized conductance observed in several experiments on transport of electrons through a QPC when we take the leads to be Fermi liquids with $K_L=1$.

We now give the expressions for the Green's functions for the case when both x and x' are taken equal to a at a point in the left contact:

$$G_{\bar{\omega}}(a,a)=\frac{K_C}{2|\bar{\omega}|}\frac{\{(r-p-q-s)e^{|\bar{\omega}|d/v_C}(1+\gamma_1e^{-|\bar{\omega}|2a/v_C})-(r+p+q-s)e^{-|\bar{\omega}|d/v_C}(e^{|\bar{\omega}|2a/v_C}+\gamma_1)\}}{\{(r-p-q-s)e^{|\bar{\omega}|d/v_C}+\gamma_1(r+p+q-s)e^{-|\bar{\omega}|d/v_C}\}}, \tag{157}$$

where

$$p = e^{-|\bar{\omega}|l(\frac{1}{v_C}+\frac{1}{v_W})}(\gamma_1e^{-2|\bar{\omega}|d/v_C}(1+\frac{K_W}{K_C})+(1-\frac{K_W}{K_C}))$$

$$
\begin{aligned}
q &= e^{-|\bar{\omega}|l(\frac{1}{v_C}-\frac{1}{v_W})}(\gamma_1 e^{-2|\bar{\omega}|d/v_C}(1-\frac{K_W}{K_C})+(1+\frac{K_W}{K_C})) \\
r &= e^{-|\bar{\omega}|l(\frac{1}{v_C}+\frac{1}{v_W})}(\gamma_1 e^{-2|\bar{\omega}|d/v_C}(1+\frac{K_C}{K_W})+(\frac{K_C}{K_W}-1)) \\
s &= e^{-|\bar{\omega}|l(\frac{1}{v_C}-\frac{1}{v_W})}(\gamma_1 e^{-2|\bar{\omega}|d/v_C}(\frac{K_C}{K_W}-1)+(1+\frac{K_C}{K_W})) \\
\gamma_1 &= \frac{K_L-K_C}{K_L+K_C}.
\end{aligned} \tag{158}
$$

The results upon taking the limits corresponding to the various frequency (or temperature) regimes are given in the section where the conductance is computed for quantum wires and quantum point contacts with a junction barrier in the left contact region and we will not repeat them here.

We also give the general form of the two-point propagator $G_{\bar{\omega}}(x,y)$ for when x is a point in the right lead and y is a point in the left contact:

$$
G_{\bar{\omega}}(x,y) = \frac{2K_2}{|\bar{\omega}|}\frac{e^{|\bar{\omega}|(l+2d)(\frac{1}{v_L}-\frac{1}{v_C})}e^{|\bar{\omega}|\frac{d}{v_C}}(1+\gamma_1)^2 e^{|\bar{\omega}|(\frac{y}{v_C}-\frac{x}{v_L})}}{\{(p+q+s-r)e^{|\bar{\omega}|d/v_C}+\gamma_1(s-r-p-q)e^{-|\bar{\omega}|d/v_C}\}}\ , \tag{159}
$$

where the expressions for p, q, r, s and γ_1 have already been given earlier.

Now, we give the expression for the one-point propagator at a point a inside the quantum wire:

$$
G_{\bar{\omega}}(a,a) = \frac{K_W}{2|\bar{\omega}|}\frac{(je^{|\bar{\omega}|a/v_W}+ke^{-|\bar{\omega}|a/v_W})(me^{|\bar{\omega}|a/v_W}+ne^{-|\bar{\omega}|a/v_W})}{(jn-km)}, \tag{160}
$$

where

$$
\begin{aligned}
j &= (1+\frac{K_W}{K_C})e^{|\bar{\omega}|d(\frac{1}{v_C}-\frac{1}{v_W})}+\gamma_1(1-\frac{K_W}{K_C})e^{-|\bar{\omega}|d(\frac{1}{v_C}+\frac{1}{v_W})} \\
k &= (1-\frac{K_W}{K_C})e^{|\bar{\omega}|d(\frac{1}{v_C}+\frac{1}{v_W})}+\gamma_1(1+\frac{K_W}{K_C})e^{-|\bar{\omega}|d(\frac{1}{v_C}-\frac{1}{v_W})} \\
m &= (1-\frac{K_W}{K_C})e^{-|\bar{\omega}|(l+d)(\frac{1}{v_C}+\frac{1}{v_W})}+\gamma_1(1+\frac{K_W}{K_C})e^{-|\bar{\omega}|(l+d)(\frac{1}{v_C}+\frac{1}{v_W})}e^{-2|\bar{\omega}|\frac{d}{v_C}} \\
n &= (1+\frac{K_W}{K_C})e^{-|\bar{\omega}|(l+d)(\frac{1}{v_C}-\frac{1}{v_W})}+\gamma_1(1-\frac{K_W}{K_C})e^{-|\bar{\omega}|(l+d)(\frac{1}{v_C}-\frac{1}{v_W})}e^{-2|\bar{\omega}|\frac{d}{v_C}}.
\end{aligned} \tag{161}
$$

Again, we will not give the results of taking the various limits corresponding to the different frequency (or temperature) regimes as these have already been quoted in the section on the conductance of a quantum wire and quantum point contact.

References

[1] S. Datta, *Electronic transport in mesoscopic systems* (Cambridge University Press, Cambridge, 1995); *Transport phenomenon in mesoscopic systems*, edited by H. Fukuyama and T. Ando (Springer Verlag, Berlin, 1992); Y. Imry, *Introduction to Mesoscopic Physics* (Oxford University Press, New York, 1997).

[2] B. J. van Wees, H. van Houten, C. W. J. Beenakker, J. G. Williamson, L. P. Kouwenhoven, D. van der Marel and C. T. Foxon, Phys. Rev. Lett. **60**, 848 (1988); D. A. Wharam, T. J. Thornton, R. Newbury, M. Pepper, H. Ahmed, J. E. Frost, D. G. Hasko, D. C. Peacock, D. A. Ritchie and G. A. C. Jones, J. Phys. C **21**, L209 (1988).

[3] S. Tarucha, T. Honda and T. Saku, Sol. St. Comm. **94**, 413 (1995).

[4] A. Yacoby, H. L. Stormer, N. S. Wingreen, L. N. Pfeiffer, K. W. Baldwin and K. W. West, Phys. Rev. Lett. **77**, 4612 (1996).

[5] K. J. Thomas, J. T. Nicholls, M. Y. Simmons, M. Pepper, D. R. Mace and D. A. Ritchie, Phys. Rev. Lett. **77**, 135 (1996).

[6] B. E. Kane, G. R. Facer, A. S. Dzurak, N. E. Lumpkin, R. G. Clark, L. N. Pfeiffer and K. W. West, App. Phys. Lett. **72**, 3506 (1998).

[7] C.-T. Liang, M. Pepper, M. Y. Simmons, C. G. Smith and D. A. Ritchie, Phys. Rev. B **61**, 9952 (2000).

[8] C.-T. Liang, M. Y. Simmons, C. G. Smith, D. A. Ritchie and M. Pepper, App. Phys. Lett. **75**, 2975 (1999).

[9] R. de Picciotto, H. L. Stormer, A. Yacoby, L. N. Pfeiffer, K. W. Baldwin and K. W. West, Phys. Rev. Lett. **85**, 1730 (2000).

[10] M. A. Topinka, B. J. LeRoy, S. E. J. Shaw, E. J. Heller, R. M. Westervelt, K. D. Maranowski and A. C. Gossard, Science bf 289, 2323 (2000).

[11] R. Crook, C. G. Smith, M. Y. Simmons and D. A. Ritchie, cond-mat/9909017.

[12] D. J. Reilly, G. R. Facer, A. S. Dzurak, B. E. Kane, R. G. Clark, P. J. Stiles, J. L. O'Brien, N. E. Lumpkin, L. N. Pfeiffer and K. W. West, cond-mat/0001174.

[13] F. D. M. Haldane, Phys. Rev. Lett. **47**, 1840 (1981).

[14] C. L. Kane and M. P. A. Fisher, Phys. Rev. B **46**, 15233 (1992).

[15] A. Furusaki and N. Nagaosa, Phys. Rev. B **47**, 4631 (1993).

[16] I. Safi and H. J. Schulz, Phys. Rev. B **52**, 17040 (1995).

[17] D. L. Maslov and M. Stone, Phys. Rev. B **52**, 5539 (1995); V. V. Ponomarenko, *ibid.* **52**, R8666 (1995).

[18] A. Furusaki and N. Nagaosa, Phys. Rev. B **54**, 5239 (1996).

[19] A. Yu. Alekseev and V. V. Cheianov, Phys. Rev. B **57**, 6834 (1998).

[20] For a review, see S. Rao and D. Sen, cond-mat/005492.

[21] M. Büttiker, Phys. Rev. B **41**, 7906 (1990).

[22] M. Fabrizio and A. O. Gogolin, Phys. Rev. B **51**, 17827 (1995).

[23] C. de C. Chamon and E. Fradkin, Phys. Rev. B **55**, 4534 (1997); N. P. Sandler, C. C. Chamon and E. Fradkin, Phys. Rev. B **56**, 2012 (1997).

[24] I. Safi and H. J. Schulz, Phys. Rev. B **59**, 3040 (1999); I. Safi, Ph.D. thesis, Laboratoire de Physique des Solides, Orsay (1996); I. Safi, Ann. Phys. (Paris) **22**, 463 (1997).

[25] K. A. Matveev, Phys. Rev. B **51**, 1743 (1995).

[26] A. Yacoby and Y. Imry, Phys. Rev. B **41**, 5341 (1990).

[27] D. L. Maslov, Phys. Rev. B **52**, R14386 (1995).

[28] T. Kimura, K. Kuroki and H. Aoki, Phys. Rev. B **53**, 9572 (1996).

[29] O. A. Tkachenko, V. A. Tkachenko, D. G. Baksheyev, C.-T. Liang, M. Y. Simmons, C. G. Smith, D. A. Ritchie, G.-H. Kim and M. Pepper, cond-mat/0003021.

[30] V. Senz, T. Heinzel, T. Ihn, S. Lindemann, R. Held, K. Ensslin, W. Wegscheider and M. Bichler, cond-mat/0012205.

Figure Captions

1. Schematic diagram of the model showing the lead regions (marked FL for Fermi liquid), the contact regions (C) of length d, and the quantum wire (QW) of length l. The interaction parameters in these three regions are denoted by K_L, K_C and K_W respectively.

2. Diagram showing the Fermi energy E_F (with a thermal spread of k_BT) in relation to the sub-bands within the quantum wire. The conductance will lie on a plateau if the energy levels are as shown in (a), while the conductance will be at a step between one plateau and the next if the energy levels are as shown in (b).

3. A plot showing the curve fitted to the conductance corrections δg versus temperature T data obtained from the inset of Fig. 3 of Yacoby *et al* [4]. The expression for the curve and the value of the correlation coefficient are given in the text.

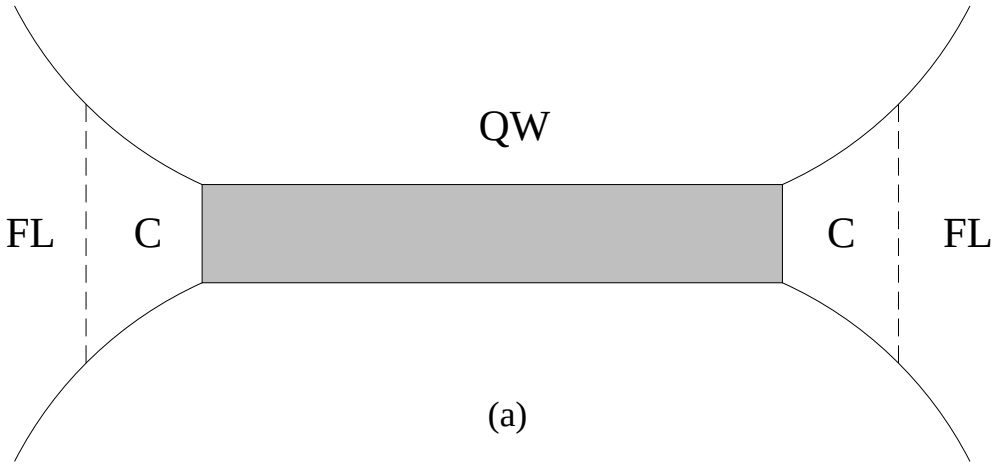

(a)

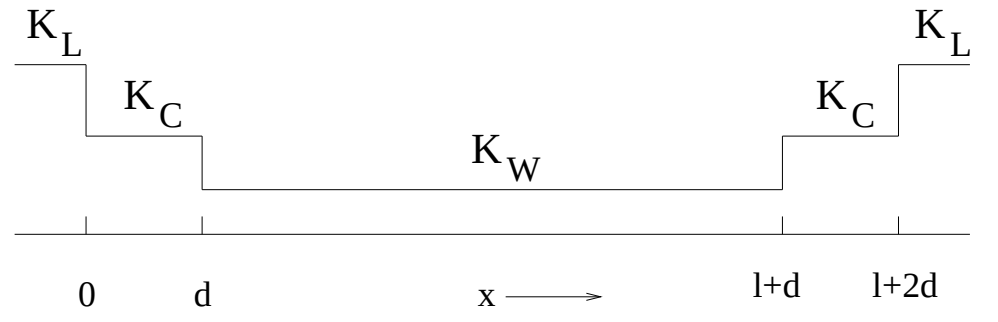

(b)

Fig. 1

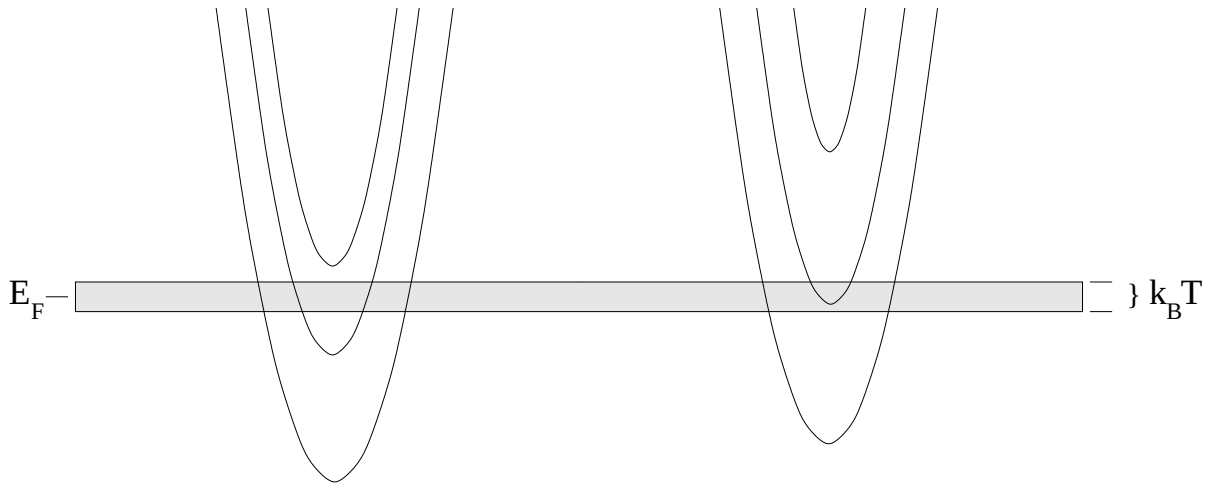

Fig. 2

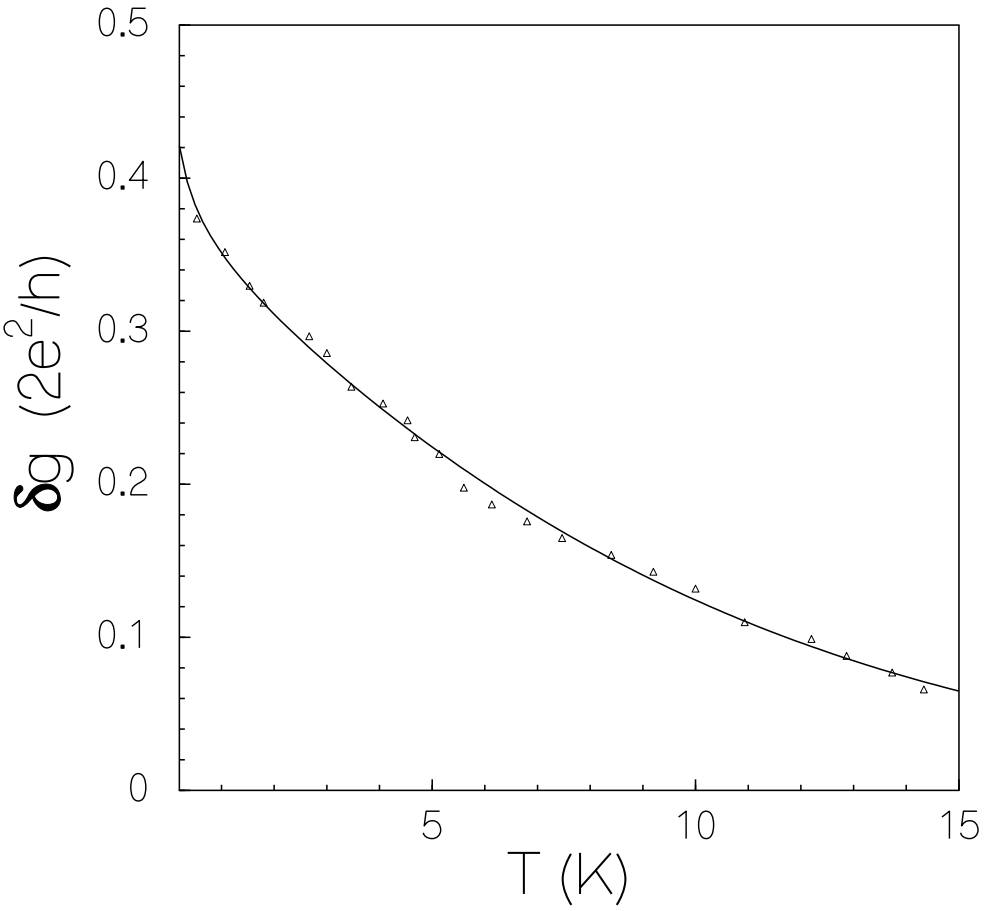

Fig. 3